

Interactions of Atmospheric Gases and Aerosols with the Monsoon Dynamics over the Sudano-Guinean region during AMMA

Adrien DEROUBAIX, Cyrille FLAMANT, Laurent MENUT, Guillaume SIOUR, Sylvain MAILLER, Solène TURQUETY, Régis BRIANT, Dmitry KHVOROSTYANOV and Suzanne CRUMEYROLLE

Dear Editor,

We thank you and the reviewers for their positive comments and opinions. About their comments, we propose in the following some answers and corrections of the manuscript.

1 Report 1

1.1 General Description of manuscript and General Comments

The authors use observations from the West Africa AMMA aircraft campaign in 2006 and an atmospheric chemistry model to diagnose the transport patterns and contributing sources to enhancements in carbon monoxide and PM 2.5 along a latitudinal transect from the Gulf of Guinea to the Sahel.

As presented currently the study appears anecdotal. It is not apparent that the features observed along a very limited longitudinal domain in West Africa apply to the rest of West Africa and to other years. Please clarify whether the findings in this study are generally applicable to the rest of West Africa and other years? If so, what do the outcomes from this study mean for past/present/future atmospheric composition or development of air quality and/or climate policy?

The present analysis is meant to be a case study for the year 2006, making use of the wealth of observations acquired during the AMMA programme. The interannual variability has not been investigated and is out of the scope of this paper. We revisited the AMMA 2006 observations to focus on the transport patterns and sources of carbon monoxide and PM2.5 over Southern West Africa, a region that has received less attention than the Sahel during AMMA.

We suspect that some of the features observed occur year after year over Southern West Africa monsoon but we cannot extrapolate from the results of our study. Here, we proposed a new approach focusing on two major pollutants (Carbon monoxide, CO, and fine atmospheric particulate matter, PM2.5) that can be transported far from the sources due to their long lifetime. They are certainly of paramount importance for air quality and climate policies development, but we feel that additional simulations are needed to address this, which is also beyond the scope of the paper.

Why not also compare the model to other parameters measured during the AMMA campaign to assist in interpreting transport patterns and contributing sources and diagnosing what causes differences between modeled and observed PM 2.5 and CO? These could include measure components of PM 2.5 (sulfate, ammonium, organic aerosol, nitrate), and CO precursor VOCs, for example.

We decided to focus on these two important atmospheric components (Carbon monoxide, CO, and fine atmospheric particulate matter, PM2.5) because the data were available. Aerosol Mass Spectrometer data were not available. For CO, we assume that we modeled the two main sources (i.e. Anthropogenic and biomass burning). Given the amount of VOCs, i.e. > 15 ppb according to Ancellet et al. (2011), VOCs oxidation must be very low (a few ppb).

1.2 Specific Comments

We thank the reviewer for taking the time to go through the spelling and grammar of the manuscript. All proposed corrections have been taken into account in the revised version of the manuscript. Below, we provide answers to the more science oriented questions the referee has.

p. 2, Lines 17-18: The authors point to economic growth as a driver of emissions from industries, including gas flaring, but the reference they site does not mention economic growth as a driver.

The sentence has been changed: *'However, the economic growth over the region drives up anthropogenic emissions: the increase of industries including gas flaring (Asuoha and Osu, 2015), of local fuel-wood burning*

for stoves and of traffic (Lioussse et al., 2010; Hadji et al., 2012; Lioussse et al., 2014) with more two-wheel vehicles using very poor fuel quality used (Ndoke and Jimoh, 2005; Assamoi and Lioussse, 2010), which are suspected to quickly worsen the air quality.'

p. 2, Line 19: Do the authors mean 'air quality standards' or air quality guidelines? If from WHO these should be guidelines.

Corrected

p. 3, lines 9-12: Presumably DACCIIWA will also contribute to understanding the change in atmospheric composition due to increases in emissions over a rapidly growing region?

The sentence has been changed: *It will contribute to understanding the change in atmospheric composition due to increases in emissions over a rapidly growing region as well as the development of the next generation of accurate models to forecast weather and pollution in southern West Africa (Knippertz et al., 2015).*

p. 3, line 31: Is a 1 month spin-up sufficient for carbon monoxide output from a model, when CO has a lifetime of 2 months?

As for all chemical species, and the principle of an area limited domain model, the lifetime of the species is not a constraint. The 'aged' concentrations are already modeled with the global climatological model, providing hourly boundary conditions. These concentrations are injected into our regional model depending on the wind direction and speed. The 'fresh' concentrations are explicitly hourly emitted in the domain.

The real constraint motivating the use of a spin-up time is the transport of the species into the domain: we want to ensure that for the first modeled hour, all possible species, due to a previous transport, are well present in the domain. There is no link to the lifetime, but depends on the transport and the domain size only.

p. 5, lines 22-23: Please point out the features that are similar to the Flaounas et al. (2010).

The paragraph related with Flaounas et al. (2010) has been modified such as: *'During this period, the precipitation location and rate will play a crucial role on the modeled surface PM_{2.5} concentrations. As a validation for this variable, the methodology of Flaounas et al. (2010) is used: precipitation rates are averaged between 8.5W and 8.5E. Day-to-day variability is smoothed by applying a moving average of ± 2 days. Figure 2 is directly comparable to the Flaounas et al. (2010) study using the same period and averaged region. In May and June, observed and modeled precipitations occur mainly over the ocean (below 5N). From late June on, the main precipitation areas move over the continent (above 5N) and reach the Sahel (at about 13N). Figure 2 shows that the modeled precipitation spatial patterns are in good agreement with the two satellite observations (TRMM and GPCP) presented in their study (see Figure 3 of Flaounas et al. (2010)).'*

p. 6, line 14: Remove parentheses around the AERONET URL.

p. 6, line 15: Space between number and units (400 nm instead of '400nm').

p. 6, line 15: Provide units for '440-870'.

p. 10, line 17: 'analyzes' should be analysis.

All four points have been corrected.

p. 10, lines 26-27: Point out in Figure 5 the feature that indicates the arrival of the cold tongue.

This sentence has been revised: *At the end of the period, when precipitation occurs inland and anth-PM_{2.5} is low, the meteorological situation changes suddenly over the ocean showing the cold tongue arrival located at the Equator, which is associated with increased wind speed between the Equator and the coast, as detailed by Meynadier et al. (2016).*

p. 12, line 31: Fix units.

p. 14, line 11: 'perturbated' should be perturbed.

p. 15, line 5 (bottom of page): Dust is repeated.

All three points have been corrected.

p. 15, line 14: What does 'Figure ??' refer to? Is this Figure 11? Indicate on the figure the convective cell.

Thanks for picking this up. Yes indeed, we meant Figure 12 (previously 11). A red ellipse has been superimposed on Figure 12 to indicate the location of the convective cell.

p. 16, lines 29-30: There is no context for why the results in this work will be compared to DACCIWA. What new insights will be gained from this comparison that justify mentioning it here?

This sentence has been changed: *Concerning air quality and climate policy development, we have shown that the export of anthropogenic pollutant from the Guinean coast toward the North could lead to cross boundary pollution plumes. This result will be confirmed by comparing to the 2016 DACCIWA campaign observations in order to propose strategy to reduce the atmospheric pollution in West Africa.*

Figures:

Figure 3: What are the statistics in the first and third panel? Does this compare the modeled component to total AOD from the measurements? Whats the value in showing this? Why not just compare total modeled and observed AOD? The label for the modeled AOD components is confusing. The label is 'AOD Anthr.' and 'AOD Fires', but shouldnt is rather be biomass burning and all other components for clarity? The figure caption suggests this is what is shown.

There is no value to keep the statistics because the scores are very slightly improved by adding biomass burning emission. It has been removed. Concerning the legend, the labels ('AOD Anthr.' and 'AOD Fires') have been replaced (by 'with biomass burning' and 'without biomass burning'). The new figure is presented below (Figure 1 of this document).

Moreover, a detailed explanation of how the different contributions are obtained has been added in Section 2.2.

2 Report 2

2.1 General Comments

This paper looks at the contribution of different emissions sources to CO and PM2.5 over W. Africa and the meteorological conditions that influence the transport of the pollutants within this region. It is a model study using a WRF coupled to CHIMERE and evaluated using measurements made during the AMMA project in 2006. It is the impact of the meteorological conditions on pollution concentrations particularly on the coastal region where the majority of people live that provides novel insight that is worthy of publication. I do have a few concerns that I would like to see addressed before publication.

2.2 Specific Comments

It is not clear to me why in section 3.3, the model meridional simulation of CO and PM2.5 is evaluated against just two flights the on consecutive days (13-14 June), during which an MCS passes through the area (section 3.3.1). On the back of this the model is then used to quantify the modelled pollution source apportionment on a monthly basis. Why not evaluate the model over the whole month? There were flights on other days and with other aircraft. There are several papers published from the AMMA campaign that could have been used to help with this evaluation see Reeves et al (2010) (www.atmos-chem-phys.net/10/7575/2010/) that gives an overview of the chemical and aerosol characterisation and references therein. Satellite data could also be used for the evaluation. This would also help to evaluate the transport of biomass burning plumes into the region from south of the aircraft flight tracks.

The section 3.3 deals with modeled and observed CO and PM2.5 during two meridional flight trajectories on consecutive days (13-14 June) because it provides data from the coast to the Sahel, thus it fits exactly the scope of the study focusing on the Sudano-Guinean region. New insights are presented gained from the AMMA 2006 observations as we focus on the transport patterns and sources of CO and PM2.5 over the Sudano-Guinean region.

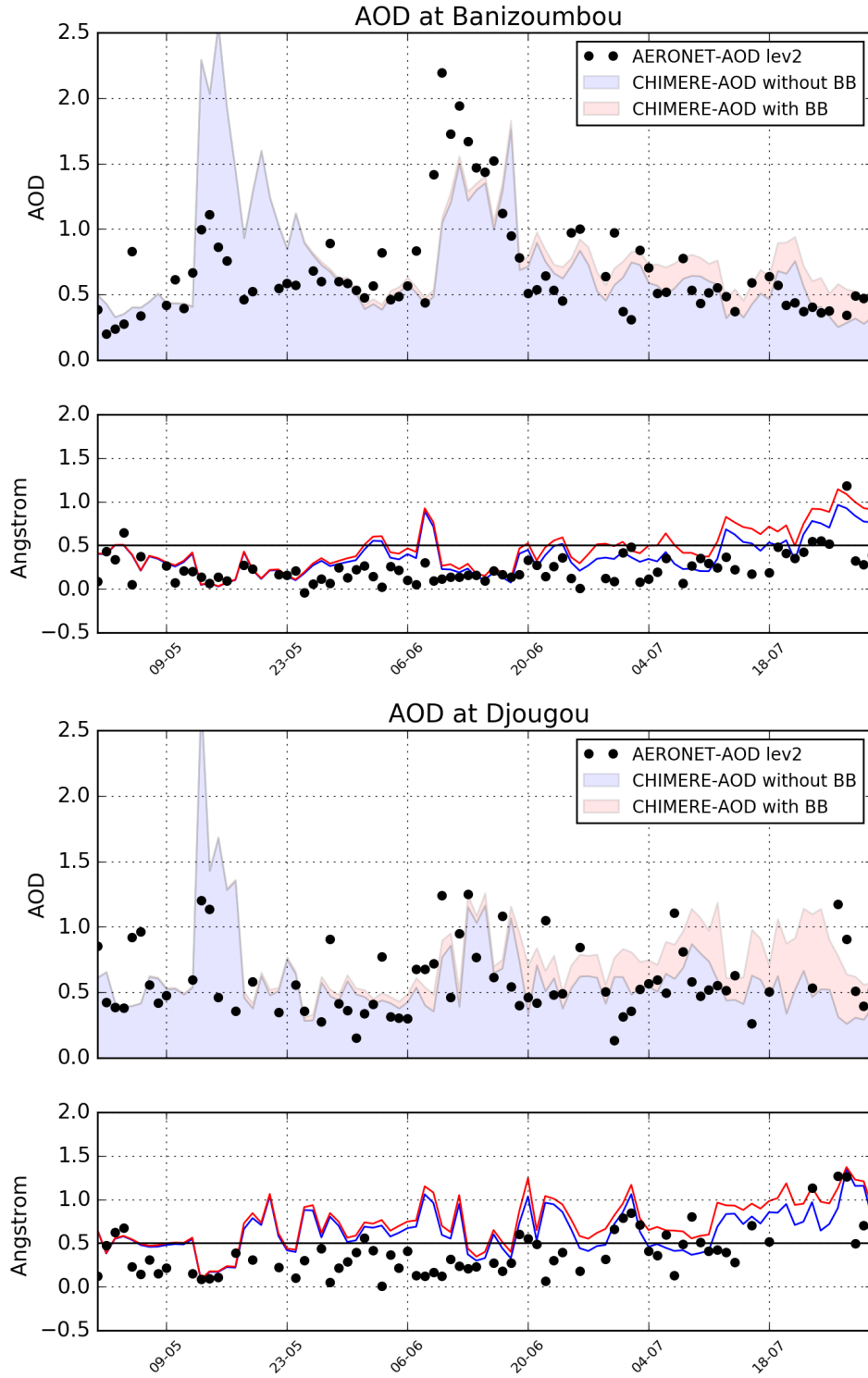


Figure 1: Observed daily averages of AERONET level 2 AOD and Angström exponent (black dots) at Djougou (Benin) and Banizoumbou compared to the modeled time series with a splitting to extract the relative contribution between without biomass burning emissions (including anthropogenic, biogenic, sea salt and mineral dust; all four in blue) and with biomass burning emissions (in red).

Moreover, it has been difficult to work with validated data from the AMMA database. Many datasets used in preliminary evaluations were partly unusable after contacting responsible people of the dataset. We have contacted FAAM team (Graeme NOTT) for data from the BAe 146 of the 20-21 July but it was not possible to produce PM concentration because: 'during this period no calibration of the PCASP was carried out by FAAM' and in the FORTRAN code, a mistake has been done using constant flow rate. Suzanne CRUMEYROLLE has provided the only aircraft data that we are confident but aerosol speciation was not available. The two flights used in our study are meridional transects that fit exactly with the purpose of the study.

How is the source apportionment (Section 3.3.1) determined? Are separate CO tracers used for the background, anthropogenic and biomass burning? How is this done for PM2.5, in particular considering how the aerosol scheme works? How is the formation of SOA considered? What about mixed aerosols? One of the main scientific questions addressed in this paper is the contribution of different sources to pollutant concentrations, so it is essential that a clear description of the methodology for determining this is included in the paper. Much of the analysis in the paper focuses on anth-PM2.5 so it must be clear how this is defined.

References describing how the aerosol scheme works in the CHIMERE model were missing in the manuscript. In the revised version of the manuscript, we now describe it as well as how the source apportionment is determined for CO and for PM2.5, which has been added in Section 2.2:

'Menut et al. (2016) have detailed and analyzed aerosol speciation and size distribution in the CHIMERE model during the summer 2013 over Europe and Africa using the AERONET network for AOD and EMEP network for PM concentrations. For the AOD calculation, the aerosol optical scheme in the CHIMERE model considers mixed aerosols following the 'core-shell' hypothesis detailed in Péré et al. (2009) and evaluated in Péré et al. (2010).

In order to quantify the PM2.5 source apportionment, we assume that it is possible to split aerosols in different families depending on the sources because their chemical compositions are different: Mineral, Biogenic, Salt and Anthropogenic. Given that anthropogenic and biomass burning aerosols have similar compositions, we have done two simulations with and without biomass burning emissions to split their contributions. The gas phase chemical scheme for SOA formation explained in Bessagnet et al. (2010) takes into account three anthropogenic and three biogenic hydrophilic species, three hydrophobic species with different saturations, and two surrogate compounds for the isoprene oxidation products.

The source apportionment has been determined for CO considering three main contributors (anthropogenic sources, biomass burning sources and long-range transport). Consequently, three simulations have been done: one without any emission source in the domain for the background concentration, one with the anthropogenic emission only, and a last one with the anthropogenic and biomass burning emissions.'

Section 4.22. I really do not understand the conclusions here. In Figure 7, surely a and b are the wrong way around, with the top plot having the 1 a.u. contour at around 7N near Cotonou and the bottom plot having it at 14N near Niamey? Perhaps I am getting muddled by this figure, but it seems extremely odd that the ratio of the coastal to Sahelian tracer is greater in the Sahelian region, especially since the tracer experiment uses arbitrary units and so does not consider the relative strengths of the tracer emissions in each region. The clarity of the discussion could be improved by attention to the English, but I think there is something scientifically wrong here.

We thank the reviewer for reporting this mistake. In this Figure (now Figure 8), a) and b) were the wrong way around. This has been corrected.

Real anthropogenic emissions represent the amount of what each city emits: their magnitude is thus representative of each location, the activity sectors and the population. After emissions, pollutants are transformed by transport, mixing, deposition and chemistry. In this case, and if we want a realistic estimate of a concentration far from the sources, it is necessary to have emissions really representative of the size of each urbanized area. The problem is different with the tracers: we don't want to have a realistic value, but just to know the percentage of what arrived at a remote location. Thus, we need to emit the same amount at every location to have the exact percentage at the studied remote location. This enables to quantify that in Niamey, Cotonou tracer concentration is about 9% (of the 1 a.u. isocontour presented in Figure 8-a), while in Cotonou, Niamey tracer concentration is about 0.03% (of the 1 a.u. isocontour presented in Figure 8-b).

In Section 4.2.2, a sentence has been added for clarity: *'The tracer experiment uses arbitrary units and considers the same quantity of tracers emitted in each town.'*

The second paragraph of this section has been changed: *'Tracers emitted at the coast indicate that there is an important transport of coastal pollutants toward the North in the PBL. On the other hand, there is no significant transport of tracers emitted in the Sahel toward the coast. In Niamey, Cotonou tracer concentration is about 9% (of the 1 a.u. isocontour presented in Figure 8-a), while in Cotonou, Niamey tracer concentration is about 0.03% (of the 1 a.u. isocontour presented in Figure 8-b). In the HTAP anthropogenic inventories (presented in Figure 1), the anth-PM_{2.5} (respectively anth-CO) is ≈ 103 (735) kg.km⁻².day⁻¹ in Niamey and ≈ 438 (7707) kg.km⁻².day⁻¹ in Cotonou. Therefore, an important part of the pollution over the Sahel has been emitted at the coast and it contributes to a maximum of anthropogenic pollution in June over the Sahel. In conclusion, the high concentration over the Sahel is due to the existence of a meridional atmospheric cell, which acts at accumulating pollutants emitted locally and remotely at the coast.'*

P 2, l 22-24: Several values are given for high concentrations of pollutants in these 3 lines. It would be helpful to give the time averages over which these measurements were made as the context of this paragraph is to compare them with the air quality standards which are for specified periods of exposure.

Time averages have been added: *'based on half-hour averages' for Baumbach et al. (1995); 'based on 1-min averages' for Dionisio et al. (2010); 'based on daily averages' for Boman et al. (2009)*

P 4, l 24-25: I'd like to see more details on how WRF is coupled to CHIMERE. Is the CHIMERE transport used or just the chemistry? Time steps for physical processes and chemistry?

In this study, we present offline simulations (CHIMERE is forced by WRF). For chemistry and aerosol simulations, the concentrations are calculated using the chemistry, transport, mixing and deposition equations implemented in the CHIMERE model. For clarity, two sentences have been added: *'The WRF and CHIMERE models are run offline on the same horizontal grids for the continental and regional domains' and 'The time step is set to 10 minutes for the physical processes and 5 minutes for the chemistry, which could change depending on the Courant-Friedrichs-Lewy condition.'*

P 5, l 24: It would be good to show plots of the TRMM and GPCP data to demonstrate the good agreement.

These two plots have been presented by Flaounas et al. (2010) as well as the comparison to the different WRF parametrization. We do not aim at focusing on the precipitation patterns in the present study. We have specifically pointed out comparable patterns of our Figure 2 and Figure 3 of Flaounas et al. (2010). The first paragraph of Section 3.1 has been modified such as: *'During this period, the precipitation location and rate will play a crucial role on the modeled surface PM_{2.5} concentrations. As a validation for this variable, the methodology of Flaounas et al. (2010) is used: precipitation rates are averaged between 8.5W and 8.5E. Day-to-day variability is smoothed by applying a moving average of ± 2 days. Figure 2 is directly comparable to the Flaounas et al. (2010) study using the same period and averaged region. In May and June, observed and modeled precipitations occur mainly over the ocean (below 5N). From late June on, the main precipitation areas move over the continent (above 5N) and reach the Sahel (at about 13N). Figure 2 shows that the modeled precipitation spatial patterns are in good agreement with the two satellite observations (TRMM and GPCP) presented in their study (see Figure 3 of Flaounas et al. (2010)).'*

P 6, l 3-8: Looking at Fig. 2, it seems to me that the precipitation is focused at 2N through much of June and that it is only until mid-late June that it shifts to more to 5N. This is not consistent with the text that says the pre-onset occurs in May.

The section 3.1 has been modified to be consistent with the figure and the three periods defined (see above).

P 9, l 30: The high CO concentrations at the coast are not so continuous in late June and July.

'during the whole period' has been changed to *'from the beginning of May to late June'*

P 10, l 5-8: Please explain more clearly how precipitation/convection impacts surface CO concentrations. How does it affect the vertical distribution?

In this section, we identify the changes which are analyzed in the following. The sentence: *'In July, the variability is mostly consistent with precipitation rates after the onset, which suggest that surface versus vertical distribution has changed by the convection associated with large scale precipitation.'* has been replaced by *'In July, the variability is mostly consistent with precipitation rates after the onset, suggesting modifications of transport and deposition patterns by the convection associated with large scale precipitation.'*

P 10, l 15-16: A cant make out any great difference between the pattern at 12N and 13N.

'at 12N' has been removed. This sentence was unclear because we were not comparing 12N and 13N. This paragraph has been modified (see above).

P 12, l 27: Are diurnal patterns included in the emission inventories used?

'when the convection and NLLJ are weak' has been removed because diurnal patterns of anthropogenic pollution are mostly driven by diurnal variation of the emissions.

P 12, l 29-31: In Fig. 8 some of the pollution over the sea on the 10-11 June in the Hovmuller plot appears to progress northwards with time (i.e. bottom left towards top right) rather than be transported out to sea from the land. Fig. 9 suggests it may be coming from other cities further to the south.

This paragraph has been modified such as: *'There is a transition from low to high concentration of anthropogenic pollution from 8 to 12 June. Anthropogenic pollution is modeled over the sea from 10 to 11 June. It is interesting to note that precipitation occurs inland on 11 June (between 18 UTC and 00 UTC), then high modeled concentrations persist during the night of 11-12 June. This precipitation event reflects a change in the wind patterns, which induces a change in the transport of pollutants, leading to surface concentrations up to 8 $\mu\text{g.m}^{-3}$ in Cotonou.'*

P 13, l 33: How can you be sure that the plumes are 'overlaying' and not mixed?

You are right, it is mixed. We are analyzing the surface level. If the tracers associated to the different cities are at the same location, it means that the pollution from the different cities is mixed.

The English needs to be improved. I have listed some places where the understanding is not clear or incorrect because of the English, but there are many minor corrections that need to be made (e.g. the appropriate use of 'the' and 'a', use of singular and plural) that I have not listed.

2.3 Technical Comments

Ensure the initial letters of 'Guinean Gulf' are in uppercase, here and throughout the paper.

OK

P 1, l 5-6: It needs to be clear what the 38% relates to. 38% of PM_{2.5}?

This sentence has been modified from *'For PM_{2.5}, desert dust decreases from $\approx 38\%$ in May to $\approx 5\%$ in July;'* to *'Desert dust decreases from $\approx 38\%$ in May to $\approx 5\%$ in July of PM_{2.5} concentration'*

P 1, l 9-10: It is not clear. Are the pollutants emitted near the coast concentrated in the Sahel?

In order to be clear, this sentence has been split in two sentences: *'Air masses dynamics concentrate pollutants emitted in the Sahel due to a meridional atmospheric cell. Moreover a part of the pollution emitted remotely at the coast is transported and accumulated over the Sahel.'*

P 1, l 11: 'Refining the analysis' reword the English. Suggest 'Focusing the analysis'

OK

P 1, l 13: 'overlay' each other?

They are mixed and not overlaying. Corrected

P 1, l 13: 'high pollution level' is ambiguous. High concentrations? High altitude?

Indeed 'level is ambiguous. It should be either 'concentration' or 'altitude'. The manuscript has been entirely modified to remove this ambiguity.

P 2, l 2: 'washout the atmosphere' change to 'wash pollutants out of the atmosphere'

OK

P 2, l 4: 'air pollution'. Are natural components of the atmosphere pollutants? E.g. Sea salt aerosols?

'air pollution sources' has been replaced by 'aerosol and gas sources'

P 2, l 7: 'in megacities' should be 'from megacities'.

OK

P 2, l 31: 'since the last decade'. The English is not clear. Do you mean 'since' or 'during'. Note that the main AMMA campaign was in 2006, i.e. more than a decade ago.

'since the last decade' has been deleted.

P 3, l 13: 'This article is dedicated to the pollutants transport over the Guinean Gulf coastal region and focuses on two major pollutant concentrations:'. Reword the English, 'This article focuses on transport of pollutants over the Guinean Gulf coastal region, in particular on:'

OK

P 3, l 15: Replace 'have both an' with 'both have a'.

P 3, l 17: Replace 'pollutants in the' with 'pollutants to the'.

P 3, l 23: Replace 'refines spatially' with 'focuses on'.

All last three points have been corrected.

P 3, l 27: It would be useful to provide a figure showing the 2 nested domains.

The latitudes and longitudes of the two domains are given in the beginning of Section 2. The results of the article concern only the West African region. Furthermore, we do not compare the coarse and fine resolutions. It is why we want to focus only on the regional domain (presented in Figure 1).

P 4, l 6: Replace 'hourly interpolated' with 'interpolated hourly'.

OK

P 4, l 8: 'better' than what?

The sentence has been changed and 'better' removed.

P 4, l 27-28: Replace 'The anthropogenic emissions are estimated using the HTAP v2 (Hemispheric Transport of Air Pollution) annual totals for the year 2010 by the EDGAR Team,' with 'The anthropogenic emissions are estimated by the EDGAR Team using the HTAP v2 (Hemispheric Transport of Air Pollution) annual totals for the year 2010,'

OK

P 4, l 31-32: 'Taking into account vegetation fires emission fluxes is of primary importance to simulate West African pollution (Giglio et al., 2006).' - The English needs improving.

This sentence has been modified: 'Biomass burning emission from Central Africa is of primary importance to simulate West African pollution (Giglio et al., 2006)'

P 4, l 31 P5, l2: Be consistent with terms and their combinations: 'fire', 'vegetation', 'biomass burning'. How were the two parts split?

The manuscript has been revised to use only 'biomass burning'.

Since the incomplete combustion is both included in anthropogenic inventories (local urban burning) and forests biomass burning inventories, the simulation was designed to split these two parts. It is now explained in Section 2.2

P 5, l 4: 'a new global soil and surface datasets' singular or plural?

P 5, l 4: 'a satellite-derived aeolian roughness length data' singular or plural?

This is singular because it is a unique dataset composed of two satellite retrievals.

The sentence has been modified such as: 'The mineral dust sources are obtained using the GARLAP (Global Aeolian Roughness Lengths from ASCAT and PARASOL) new global soil and surface dataset made from satellite-derived aeolian roughness lengths with a 6 km spatial resolution, as detailed in Mailler et al. (2016).'

P 5, l 14-15: 'first analyze and quantify the temporal variability of the pollutants concentrations modeled in the urbanized areas along the Guinean Gulf coast during the whole AMMA-SOP1 period (Redelsperger et al.,

2006). First' There are two 'firsts' which is confusing. It states that the temporal variability of the pollutants will be analysed, but in the rest of the paragraph I can only see mention of AOD. What about any other pollutants?

This sentence has been modified: *'In this section, we analyze the temporal variability of precipitation, gas and aerosol during the whole AMMA-SOP1 period (Redelsperger et al., 2006).'*

P 5, l 29: Replace 'interactions constituted' by 'interactions, which are made up'.

OK

P 6, l 27: Replace 'lead' with 'leads'.

OK

P 7, l 5-6: English needs improving.

'Two flights made during a 'North-South land-atmosphere-ocean interaction' mission plans have been conducted over the Cotonou-Niamey meridional transect on 13 and 14 June 2006.' has been modified such as: *'We are studying two flights conducted along a meridional transect between Cotonou and Niamey on 13 and 14 June 2006 as part of a 'North-South land-atmosphere-ocean interaction' survey mission.'*

P 7, l 28: What is meant by 'a South-North gradient is expected moving closer to the Sahara'?

'a South-North gradient is expected moving closer to the Sahara' is unclear and it has been modified such as: *'For PM_{2.5}, a South-North gradient is expected with the highest concentrations close to the Sahara.'*

P 7, l 31 and P8, l 4: What is meant by 'a gap of concentration'?

This has been replaced by: *'important increase of the concentration'*

P 7, l 7: To test if the model reproduces the MCS, why not compare modelled meteorological parameters with observed e.g. satellite precipitation.

A new figure has been added in Section 3.3.1 (presented in [Figure 2](#) of this document), which aims at presenting the meteorological situation on 13-14 June as well as validating the model meteorology. The first paragraph of this section has been modified such as: *'We are studying two flights conducted along a meridional transect between Cotonou and Niamey on 13 and 14 June 2006 as part of a 'North-South land-atmosphere-ocean interaction' survey mission. During these two days, the WAM dynamics over the area were perturbed by the presence of a MCS. It developed over the Jos Plateau (Nigeria) around 16:00 UTC, reaching the Benin-Nigeria border at 20:00 UTC and moved southwestward across Benin overnight and into central Ghana, as already described in Flamant et al. (2009) and (Crumeyrolle et al., 2011). The model reproduces the location of this MCS but earlier than in the observations, i.e. reaching the Benin-Nigeria border at 10:00 UTC (Figure 4). The MCS interacts with the dust layer coming from the Sahara (especially from the Bodele depression), changing the dust load and vertical distribution over Benin and Niger. Associated with subsidence in the wake of the MCS, there is a lowering of the dust layer height (Flamant et al., 2009).'*

P 7, l 8: Replace 'not realistic' with 'unrealistic'.

OK

P 7, l 9: Why 'Nevertheless'?

This sentence has been modified: *'Nevertheless, the order of magnitude of the CO and PM_{2.5} concentrations are good in agreement with observations.'*

P 8, l 31: Presumably by 'vegetation emissions' you mean biomass burning rather than biogenic. This needs to be clear and correct throughout the paper.

OK

P 8, l 33-34 and P 9, l 5 and 10: Units of ppb should be microg / m³.

OK

P 10, l 10: Why 'more important'?

P 10, l 11: What 'increase'? The English in this sentence needs improving. Consider splitting it in two.

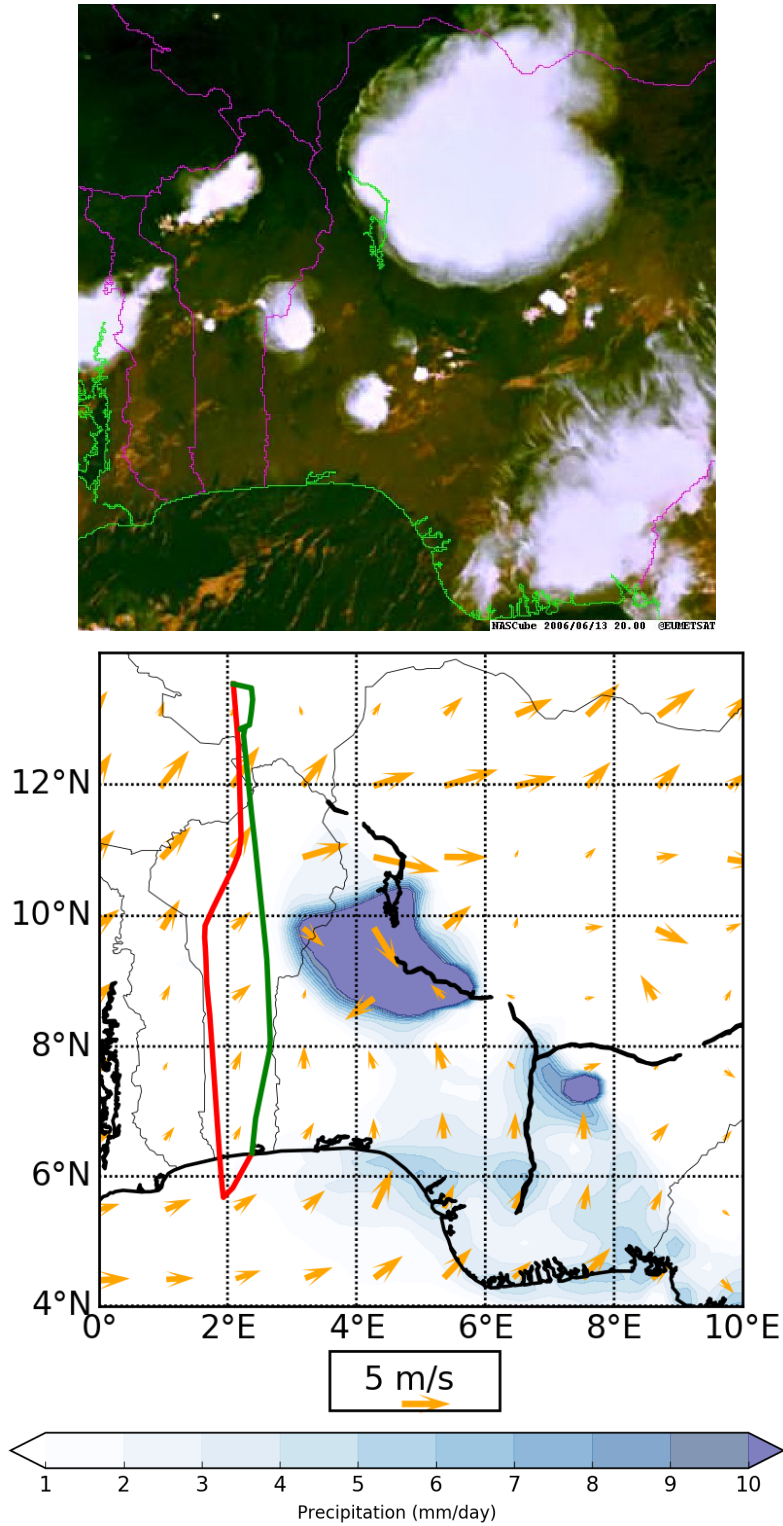


Figure 2: (top) EUMETSAT visible image of the Cotonou area of the 13 June 2006 at 20 UTC (from NAScube (<http://nascube.univ-lille1.fr>)); (bottom) Map of Cotonou area for the 13 June 2006 at 12 UTC with wind vectors at 10 m (orange arrows), precipitation (blue shading). The two flight trajectories are displayed with the red line for the 13 June and with the green line for the 14 June.

For the two last points, the sentences: *'The same behavior is observed for the surface concentrations of PM_{2.5}. The week to week variability is more important. This increase is probably due to the longer CO lifetime compared with that of PM (being less chemically active and without settling), the CO concentrations are more homogeneously mixed in a large latitudinal area from the coast to more than 16 up to the North.'*, have been reworded: *'The same behavior is observed for the surface concentrations of PM_{2.5}. The week to week variability is greater than for anth-CO, which is probably due to the longer lifetime of CO compared with that of PM (being less chemically active and less prone to settling). CO is more homogeneously mixed than PM in a large latitudinal area spanning from the coast to latitudes higher than 16.'*

P 10, l 13: A frequency has units of 1/time. Do you mean a periodicity close to 2 weeks?

OK

P 10, l 14: A wouldnt call these features plumes as they are a characteristic of a Hovmuller plot rather than a pollution plume.

'latitudinal plumes' has been replaced by: *'latitudinal patterns'*

P 11, l 19: anti-clockwise?

Yes, it has been corrected.

P 12, l 25: Replace 'derives' with 'are transported'.

OK

P 14, l 11-12: Low and high anthropogenic pollution where? Contonou?

Yes, *'in Cotonou'* has been added.

P 15, l 14: 'Figure ??', 11.

OK

Fig. 2. Caption 'regional domain' should be replaced by 'regional model domain'.

OK

Fig. 3. The legend only says 'anthr' but the captions says 'anthropogenic, biogenic and mineral dust'. Is the red line the sum of 'anthropogenic, biogenic and mineral dust' and 'biomass burning emissions'?

In red, this is anthropogenic plus biogenic plus mineral dust plus sea salt. The legend's labels ('AOD Anthr.' and 'AOD Fires') have been replaced (by 'with biomass burning' and 'without biomass burning').

Fig. 6 caption: what PM_{2.5} mass density is the light orange line meant to be? Shading should be lines.

We tried to remove shading but it leads to too much contours, which is difficult to read. In the end, we use shading for the meridional wind speed and contours for the anthropogenic PM_{2.5} concentration. The light orange line has been removed and we focus only on anthropogenic PM_{2.5} concentration = 4.0 $\mu\text{g.m}^{-3}$ (orange) and = 5.0 $\mu\text{g.m}^{-3}$ (violet). The new figure is presented below ([Figure 3](#) of this document).

Fig. 7 caption: Shading should be lines. It is not clear if one line is white or both are yellow.

As for the previous figure, we have removed the white line. The comment of this figure is now focused on only two isocontours. The new figure is presented below ([Figure 4](#) of this document).

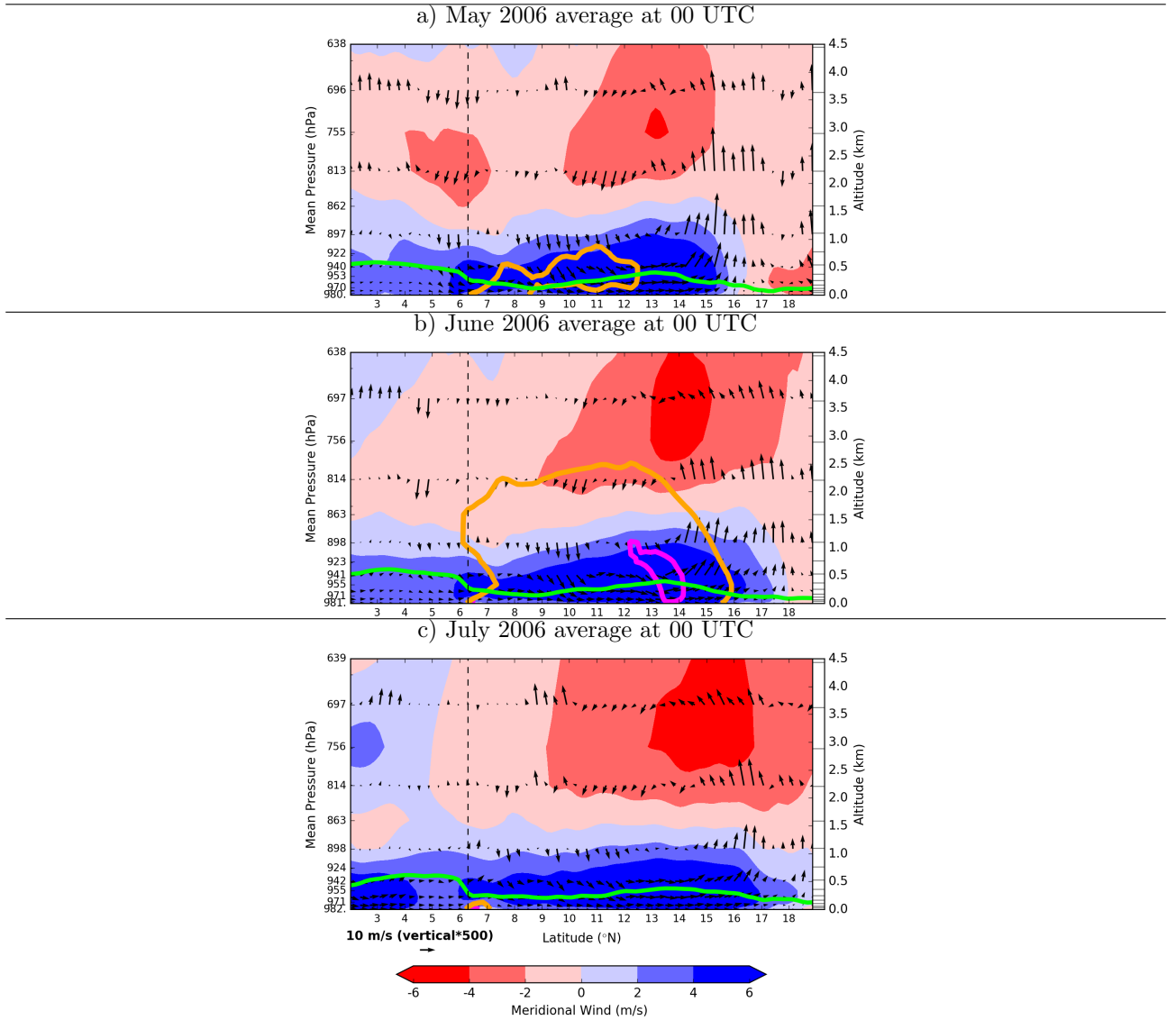
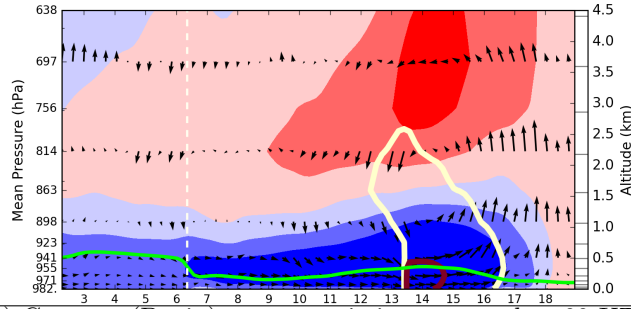


Figure 3: Vertical cross-section of the meridional wind (shading in $m.s^{-1}$) mean over: a) May, b) June and c) July, at 00 UTC along a meridional transect from 2N to 19N and averaged from 2E to 3E including Cotonou (Benin) and Niamey (Niger). Orange and violet shading represent anthropogenic $PM_{2.5}$ concentrations of $= 4.0 \mu g.m^{-3}$ and $= 5.0 \mu g.m^{-3}$. Vectors represent the wind field in the plan of the transect (with an aspect ratio of 500 between the meridional and the vertical components). The green line is the PBL height (m). The grey vertical dash line is the latitude of the coast.

a) Niamey (Niger) tracers emission averaged at 00 UTC



b) Cotonou (Benin) tracers emission averaged at 00 UTC

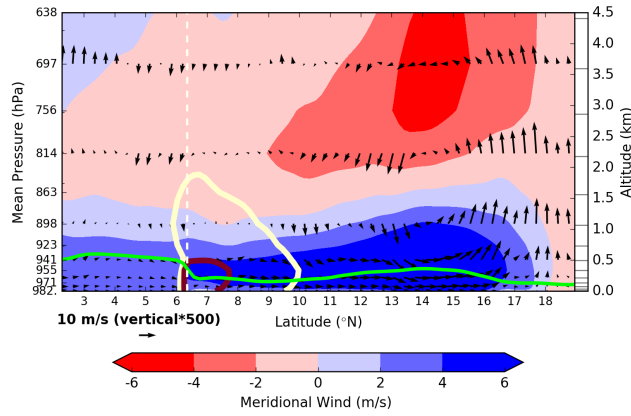


Figure 4: Vertical cross-section of the meridional wind (shading in m.s^{-1}) along a meridional transect from 2N to 19N, averaged from 2E to 3E including Cotonou (Benin) and Niamey (Niger) and averaged over 20 to 30 June at 00 UTC. Isocontours represent gaseous tracers concentration continuously emitted (in arbitrary unit) from the 1 to 30 June at: a) Niamey (Niger) and b) Cotonou (Benin). Brown and yellow shading represent tracers concentration = 1 a.u. and = 10 % a.u. respectively. The green line is the PBL height (m). Vectors represent the wind field in the plan of the transect (with an aspect ratio of 500 between the meridional and the vertical components). The white vertical dash line is the latitude of the coast.

References

- Assamoi, E.-M. and Lioussse, C. (2010). A new inventory for two-wheel vehicle emissions in West Africa for 2002. *Atmospheric Environment*, 44(32):3985–3996.
- Asuoha, A. N. and Osu, C. I. (2015). Seasonal variation of meteorological factors on air parameters and the impact of gas flaring on air quality of some cities in Niger Delta (Ibena and its environs). *African Journal of Environmental Science and Technology*, 9(3):218–227.
- Baumbach, G., Vogt, U., Hein, K. R. G., Oluwole, a. F., Ogunsola, O. J., Olaniyi, H. B., and Akeredolu, F. a. (1995). Air pollution in a large tropical city with a high traffic density - Results of measurements in Lagos, Nigeria. *Science of the Total Environment*, 169:25–31.
- Bessagnet, B., Seigneur, C., and Menut, L. (2010). Impact of dry deposition of semi-volatile organic compounds on secondary organic aerosols. *Atmospheric Environment*, 44(14):1781–1787.
- Boman, J., Lindén, J., Thorsson, S., Holmer, B., and Eliasson, I. (2009). A tentative study of urban and suburban fine particles (PM_{2.5}) collected in Ouagadougou, Burkina Faso. *X-Ray Spectrometry*, 38(April):354–362.
- Crumevolle, S., Tulet, P., Gomes, L., Garcia-Carreras, L., Flamant, C., Parker, D. J., Matsuki, A., Formenti, P., and Schwarzenboeck, A. (2011). Transport of dust particles from the Bodélé region to the monsoon layer - AMMA case study of the 9-14 June 2006 period. *Atmospheric Chemistry and Physics*, 11:479–494.
- Dionisio, K. L., Rooney, M. S., Arku, R. E., Friedman, A. B., Hughes, A. F., Vallarino, J., Agyei-Mensah, S., Spengler, J. D., and Ezzati, M. (2010). Within-Neighborhood Patterns and Sources of Particle Pollution: Mobile Monitoring and Geographic Information System Analysis in Four Communities in Accra, Ghana. *Environmental Health Perspectives*, 118(5):607–613.
- Flamant, C., Lavaysse, C., Todd, M. C., Chaboureaud, J. P., and Pelon, J. (2009). Multi-platform observations of a springtime case of Bodele and Sudan dust emission, transport and scavenging over West Africa. *Quarterly Journal of the Royal Meteorological Society*, 135(February):413–430.
- Flaounas, E., Bastin, S., and Janicot, S. (2010). Regional climate modelling of the 2006 West African monsoon: sensitivity to convection and planetary boundary layer parameterisation using WRF. *Climate Dynamics*, 36(5-6):1083–1105.
- Giglio, L., Csiszar, I., and Justice, C. O. (2006). Global distribution and seasonality of active fires as observed with the Terra and Aqua Moderate Resolution Imaging Spectroradiometer (MODIS) sensors. *Journal of Geophysical Research: Biogeosciences*, 111(2):1–12.
- Hadji, E., Doumbia, T., Lioussse, C., Galy-lacaux, C., Ababacar, S., Diop, B., Ouafu, M., Michel, E., Gardrat, E., Castera, P., Rosset, R., Akpo, A., and Sigha, L. (2012). Real time black carbon measurements in West and Central Africa urban sites. *Atmospheric Environment*, 54:529–537.
- Knippertz, P., Coe, H., Chiu, J. C., Evans, M. J., Fink, A. H., Kalthoff, N., Lioussse, C., Mari, C., Allan, R. P., Brooks, B., Danour, S., Flamant, C., Jegede, O. O., Lohou, F., and Marsham, J. H. (2015). The DACCIIWA project: Dynamics-aerosol-chemistry-cloud interactions in West Africa. *Bulletin of the American Meteorological Society*, page 150203142711003.
- Lioussse, C., Assamoi, E., Criqui, P., Granier, C., and Rosset, R. (2014). Explosive growth in African combustion emissions from 2005 to 2030. *Environmental Research Letters*, 9(3):035003.
- Lioussse, C., Guillaume, B., Grégoire, J. M., Mallet, M., Galy, C., Pont, V., Akpo, a., Bedou, M., Castéra, P., Dungall, L., Gardrat, E., Granier, C., Konaré, a., Malavelle, F., Mariscal, a., Mieville, a., Rosset, R., Serça, D., Solmon, F., Tummon, F., Assamoi, E., Yoboué, V., and Van Velthoven, P. (2010). Updated African biomass burning emission inventories in the framework of the AMMA-IDAF program, with an evaluation of combustion aerosols. *Atmospheric Chemistry and Physics*, 10:9631–9646.
- Mailler, S., Menut, L., Khvorostyanov, D., Valari, M., Couvidat, F., Siour, G., Turquety, S., Briant, R., Tuccella, P., Bessagnet, B., Colette, A., Létinois, L., and Meleux, F. (2016). CHIMERE-2016: From urban to hemispheric chemistry-transport modeling. *Geoscientific Model Development Discussions*, 0(September):1–41.

- Menut, L., Siour, G., Mailler, S., Couvidat, F., and Bessagnet, B. (2016). Observations and regional modeling of aerosol optical properties, speciation and size distribution over Northern Africa and western Europe. *Atmospheric Chemistry and Physics*, 16(20):12961–12982.
- Meynadier, R., de Coëtlogon, G., Leduc-Leballeur, M., Eymard, L., and Janicot, S. (2016). Seasonal influence of the sea surface temperature on the low atmospheric circulation and precipitation in the eastern equatorial Atlantic. *Climate Dynamics*, 47(3-4):1127–1142.
- Ndoke, P. and Jimoh, O. (2005). Impact of traffic emission on air quality in a developing city of Nigeria. *Assumpt Univ J Technol*, pages 222–227.
- Péré, J., Mallet, M., Pont, V., and Bessagnet, B. (2010). *Atmospheric Environment*, 44(30):3688–3699.
- Péré, J. C., Mallet, M., Bessagnet, B., and Pont, V. (2009). Evidence of the aerosol core-shell mixing state over Europe during the heat wave of summer 2003 by using CHIMERE simulations and AERONET inversions. *Geophysical Research Letters*, 36(9):L09807.
- Redelsperger, J. L., Thorncroft, C. D., Diedhiou, A., Lebel, T., Parker, D. J., and Polcher, J. (2006). The African Monsoon Multidisciplinary Analysis: An International Research Project and Field Campaign. *Bulletin of the American Meteorological Society*, 87(12):1739–1746.

Interactions of Atmospheric Gases and Aerosols with the Monsoon Dynamics over the Sudano-Guinean region during AMMA

Adrien DEROUBAIX^{1,2}, Cyrille FLAMANT², Laurent MENUT¹, Guillaume SIOUR³, Sylvain MAILLER¹, Solène TURQUETY¹, Régis BRIANT¹, Dmitry KHVOROSTYANOV¹, and Suzanne CRUMEYROLLE⁴

¹LMD/IPSL, École Polytechnique, Université Paris Saclay, ENS, IPSL Research University; Sorbonne Universités, UPMC Univ Paris 06, CNRS, Palaiseau, France

²LATMOS/IPSL, UPMC, Sorbonne Universités, CNRS & UVSQ, Paris, France

³LISA/IPSL, Universités Paris Est Créteil & Paris Diderot, Créteil, France

⁴LOA, Université Lille 1 Sciences et Technologies, Villeneuve d'Ascq, France

Correspondence to: Adrien Deroubaix, adrien.deroubaix@lmd.polytechnique.fr

Abstract. Carbon monoxide, CO, and fine atmospheric particulate matter, PM_{2.5}, are analyzed over the Guinean ~~gulf~~ Gulf coastal region using the WRF-CHIMERE modeling system and observations during the beginning of the monsoon 2006 (from May to July), corresponding to the Africa Multidisciplinary Monsoon Analysis (AMMA) campaign period.

Along the Guinean ~~gulf~~ Gulf coast, the contribution of long-range pollution transport to CO or PM_{2.5} concentrations is impor-

5 tant. ~~For PM~~ The contribution of desert dust PM_{2.5}, ~~desert dust concentration~~ decreases from $\approx 38\%$ in May to $\approx 5\%$ in July; ~~biomass burning aerosol~~. The contribution of biomass burning PM_{2.5} concentration from Central Africa increases from $\approx 10\%$ in May to $\approx 52\%$ in July. The anthropogenic contribution is $\approx 30\%$ for CO and $\approx 10\%$ for PM_{2.5} during the whole period. When focusing only on anthropogenic pollution, frequent northward transport events from the coast to the Sahel are associated with periods of low wind and no precipitation. In June, anthropogenic PM_{2.5} and CO concentrations are higher than in May or
10 July over the Guinean coastal region. ~~Over the Sahel, air masses~~ Air mass dynamics concentrate pollutants emitted ~~locally and remotely at the coast in the Sahel~~ due to a meridional atmospheric cell. Moreover a part of the pollution emitted remotely at the coast is transported and accumulated over the Sahel.

Refining Focusing the analysis on the period 8 - 15 June, anthropogenic pollutants emitted along the coastline are exported toward the North especially at the beginning of the night (18 UTC to 00 UTC) with the establishment of the nocturnal low
15 level jet. Plumes originating from different cities ~~overlay are mixed~~ for some hours at the coast, leading to high pollution ~~level~~ concentration, because of specific disturbed meteorological conditions.

1 Introduction

The ~~interactions~~ interaction between air pollution and climate in megacities is a challenging field of research (Baklanov et al.,
20 2016). In the countries of the Guinean Gulf, the population has been growing rapidly during the last decades, accompanied by economic development. Parallel to industrialization, air pollution is increasing without any governmental control (Zhu, 2012).

During the dry season (*i.e.* November - April), ~~when the Harmattan easterly wind is weak~~, high ozone concentrations and smog are observed over megacities such as Lagos or Cotonou ~~when the Harmattan easterly wind is weak~~ (Marais et al., 2014; Minga et al., 2009). During the wet season (*i.e.* May - October), the West African Monsoon (WAM) wind carries the pollutants northward, and local convective precipitations wash ~~out pollutants out of~~ the atmosphere. Two precipitation periods occur over
5 the Guinean Gulf coastal region in April-May and August-September. Between these two periods, the wind coming from the South is predominant (Janicot et al., 2008).

There are various ~~air pollution aerosol and gas~~ sources in the Guinean Gulf coastal region during the WAM. Sea salt aerosols are transported in the marine boundary layer, and mineral dust aerosols are transported in the Saharan Air Layer (SAL) above the monsoon air (Lafore et al., 2011). Biogenic components are emitted by tropical forests (Reeves et al., 2010), and the
10 urban air pollution ~~in megacities (Liousse et al., 2014)~~ ~~from megacities leading to ozone production (Ancellet et al., 2011)~~ (Liousse et al., 2014). In addition, pollutants resulting from incomplete combustion such as carbon monoxide and black carbon particles ~~are~~ coming from the Southern hemisphere due to biomass burning ~~reach emissions, and are reaching~~ the Guinean coast in June (Mari et al., 2007). Biomass (Mari et al., 2007) (Williams et al., 2010). In situ biomass burning plumes observations have ~~shown measured~~ high ozone (≥ 60 ppb at 700 hPa) and carbon monoxide ~~concentration~~ (≥ 200 ppb at 700 hPa)
15 ~~concentrations~~ (Sauvage et al., 2004; Mari et al., 2011).

In Nigeria, Akeredolu (1989) have listed the different sources of particle loading: biomass burning (31.7 %), fugitive dust from roads (29.1 %), fuel wood burning (21.3 %), Harmattan dust (13.8 %), solid waste incineration (2.1 %), stationary sources (1.6 %), automobile exhaust lead (0.2 %) and gas flares (0.1 %). Since the 1990's, natural ~~pollutions pollution~~ from desert dust and ~~vegetation fires remains biomass burning has remained~~ important (Mari et al., 2011; Haywood et al., 2008). However,
20 ~~anthropogenic pollution has increased: there is more the economic growth over the region drives up anthropogenic emissions; the increase of industries including gas flaring (Asuoha and Osu, 2015), of local fuel-wood burning for stoves and more of~~ traffic (Liousse et al., 2010; Hadji et al., 2012; Liousse et al., 2014) with more two-wheel vehicles ~~using very poor quality fuel~~ (Ndoke and Jimoh, 2005) (Assamoi and Liousse, 2010), which are suspected to quickly worsen ~~the air quality, partly due to the very poor fuel quality used (Ndoke and Jimoh, 2005; Ndoke and Jimoh, 2010); the economic growth over the region drives~~
25 ~~up emissions by industries including gas flaring (Asuoha and Osu, 2015) air quality.~~

All ~~studies of~~ air quality monitoring ~~studies~~ have shown that the outdoor ~~air quality standards WHO air quality guidelines~~ (*i.e.* threshold concentrations) are largely exceeded. These thresholds are for CO: 35 ppm for 1 h and 9 ppm for 8 h exposure; and for PM_{2.5}: 10 $\mu\text{g.m}^{-3}$ annual mean, 25 $\mu\text{g.m}^{-3}$ for 24-hour mean. For instance, in April 1993, Baumbach et al. (1995) have measured ~~in Lagos (Nigeria) very~~ high levels of ~~carbon monoxide, CO,~~ (up to 10 ppm, measured close to high traffic road)
30 and total particulate matter (up to 200 $\mu\text{g.m}^{-3}$) ~~based on half-hour averages in Lagos (Nigeria)~~. In Accra (Ghana), Dionisio et al. (2010) have measured PM_{2.5} up to 200 $\mu\text{g.m}^{-3}$ ~~in a polluted street (based on 1-min averages) in streets polluted~~ by wood stoves, heavy traffic and trash burning. In Ouagadougou (Burkina Faso) PM_{2.5} ~~observations (based on daily averages)~~ reach 164 $\mu\text{g.m}^{-3}$ (Boman et al., 2009) and CO concentration measured in-traffic frequently exceed all World Health Organization (WHO) guidelines (Lindén et al., 2008).

The health impact of such air pollution is expected to be high and to increase ~~further~~ without any specific emission regulation (Lindén et al., 2012). It is therefore important to gain a better understanding of ~~the pollutants'~~ pollutant emissions and transport in West Africa. All these results have highlighted the high level of pollution in megacities ~~affecting~~, affecting also remote places. However, there is no continuous air quality monitoring in West Africa, so existing studies are focused on local ~~seals~~ scales, short
5 time ~~period~~ periods, and few pollutants.

Several observation campaigns have been dedicated to ~~WAM since the last decade~~ the WAM, notably the Africa Multidisciplinary Monsoon Analysis (AMMA), which was the first international program started to improve our knowledge ~~of~~ on all aspects of the WAM (Redelsperger et al., 2006). WAM modeling made progresses, however the Guinean Gulf coastal region is challenging to model because of the complex land-sea-atmosphere interactions.

10 Along the coastline, there are several atmospheric cells acting ~~at~~ on different scales. The diurnal cycle of the land-sea breeze occurs at a local scale (a few kilometers). During the day, surface wind is linked with convection within the boundary layer, while at night there is the formation of the Nocturnal Low Level Jet (NLLJ) in response to the daily deep convection activity (Parker et al., 2005). At a regional scale (a few hundred kilometers), the monsoon wind from the South meets the Harmattan wind from the North, forming the Inter Tropical Discontinuity at ~~the~~ ground level (Flamant et al., 2007; Cuesta et al., 2009;
15 Karam et al., 2009; Pospichal et al., 2010), and leading to a complex vertical structure (Haywood et al., 2008; Lafore et al., 2011). Between these two scales, an additional meridional atmospheric cell is suspected in the low atmosphere enhancing convergence at the coast (Leduc-Leballeur et al., 2013), ~~which~~. This cell results from a gradient of wind speed due to the meridional gradient of sea surface temperature (de Coëtlogon et al., 2014). The recent research program "Dynamics-Aerosol-Chemistry-Cloud Interactions in West Africa program" (DACCIIWA) has been dedicated to the study of land-sea-atmosphere
20 interactions in West Africa. It will contribute to ~~the understanding changes in the atmospheric composition due to increasing in emissions over a rapidly growing region, as well as to the~~ development of the next generation of accurate models to forecast weather and pollution in southern West Africa (Knippertz et al., 2015).

This article ~~is dedicated to the pollutants transport~~ focuses on transport of pollutants over the Guinean Gulf coastal region ~~and focuses on two major pollutant concentrations, in particular on~~: Carbon monoxide and Particulate Matter with an aerodynamic
25 diameter $D_p < 2.5 \mu\text{m}$ (CO and $\text{PM}_{2.5}$ hereafter), which ~~have both an~~ both have a detrimental impact on health (Lelieveld et al., 2015). The scientific questions addressed in this work are:

- *What is the relative contribution of long-range transported and locally emitted pollutants ~~in the~~ to surface concentrations from the Guinean Gulf to the Sahel?*
- *What is the impact of meridional atmospheric cells on the transport of pollutants emitted from coastal megacities?*

30 The pollution patterns are analyzed during the 2006 AMMA period using several observational data sets in combination with numerical simulations of the meteorology as well as of the aerosol-gas chemistry and transport presented in ~~section~~ Section 2. Section 3 presents the main spatial and temporal patterns over the Sudano-Guinean region of the AMMA study case. Section 4 analyzes the anthropogenic pollution from the coast to the Sahel. Section 5 ~~refines spatially the analysis on~~ focuses

on the analysis of the coastal dynamics and pollution transport. Section 6 focuses on specific study cases. Conclusions and perspectives are given in ~~section~~Section 7.

2 Weather-Pollution modeling configuration

The modeling analysis was performed using the Weather Research and Forecasting (WRF) model for the meteorological fields, which drives the CHIMERE model for the gaseous and particulate species concentrations. Two nested geographical domains are defined: a continental one to take into account remote sources and long-range transport from the Mediterranean sea to the tropic of Capricorn (27°S to 44°N; 38°W to 47°E); and a regional one, centered on the Guinean Gulf (1°N to 20°N; 23°W to 17°E). The WRF and CHIMERE models ~~work are run offline~~ on the same ~~two horizontal grids~~ horizontal grids for the continental and regional domains. The simulated time period is April to ~~end of~~ July 2006, including a one month spin-up.

2.1 Meteorological fields with the WRF model

The meteorological variables are modeled with the regional non-hydrostatic WRF model (version 3.7.1) presented by Skamarock and Klemp (2008). The continental domain has a constant horizontal resolution of 60 km × 60 km, and the regional domain has a constant horizontal resolution of 20 km × 20 km ~~for the regional one~~, both with 32 vertical levels from the surface to 50 hPa. We use a 2-way nesting with the WRF model.

The global meteorological fields are taken from the US Global Forecast System produced by the National Center for Environmental Prediction. It is read and ~~hourly interpolated~~ interpolated hourly by WRF using low frequency spectral nudging above the PBL in order to enable the PBL variability to be resolved by WRF (von Storch et al., 2000). We followed the recommendations of Flaounas et al. (2010, 2011) to configure the convection and planetary boundary layer schemes ~~which have optimized a better model with a~~ set-up ~~for the entire~~ optimized for the 2006 WAM, especially for the meridional gradient of temperature and the low level circulation.

The Single Moment-6 class microphysics scheme (WSM6) is used allowing for mixed phase processes suitable for high resolution simulations (Hong and Lim, 2006). Li et al. (2015) have shown that WAM precipitation patterns are very sensitive to the radiation scheme, and the most realistic patterns were obtained with the Rapid Radiative Transfer Model for General Circulation Models (RRTMG) with the Monte-Carlo Independent Column Approximation (McICA) method of random cloud overlap from Mlawer et al. (1997). The planetary boundary layer physics are computed using the Yonsei University scheme (Hong et al., 2006). The cumulus parametrization used is the ensemble Grell-Dévényi scheme, as Crétat and Pohl (2012) have shown that internal variability is much larger with the Kain-Fritsch scheme than ~~for~~ with the Grell-Dévényi scheme at the seasonal, intra-seasonal, and daily time scales, and from the regional to the local (grid point) spatial scales. The surface layer scheme is based on Monin-Obukhov with a Carlson-Boland viscous sub-layer. The surface physics are calculated using the 'Noah' Land Surface Model ~~)-scheme~~ with four soil temperatures and moisture layers ~~Ek et al. (2003)~~ (Ek et al., 2003).

2.2 Chemistry-Transport with the CHIMERE model

CHIMERE is a regional chemistry-transport model (version 2017), fully described in Menut et al. (2013a); Mailler et al. (2016). The CHIMERE model has previously been used over the AMMA observation period but only dust aerosols were modeled (Schmechtig et al., 2011; Menut et al., 2009). In this study, all important gas and aerosol sources are included (anthropogenic, biogenic, mineral dust, sea salt and biomass burning). The 32 vertical levels of the WRF model are projected on the 20 levels for CHIMERE from the surface to 200 hPa. We use a 1-way nesting with the CHIMERE model.

The anthropogenic emissions are estimated by the EDGAR Team using the HTAP v2 (Hemispheric Transport of Air Pollution) annual totals for the year 2010 ~~by the EDGAR Team~~, using inventories based on the MICS-Asia, EPA-US/Canada and TNO databases (available at http://edgar.jrc.ec.europa.eu/htap_v2). Figure 1 presents the anthropogenic PM and CO emissions over the regional domain and the Cotonou-Niamey meridional transect used for the analysis in the next sections, defined in longitude $\lambda = 2^\circ$ East to 3° East, and in latitude $\phi = 1^\circ$ North to 19° North.

~~Taking into account vegetation fires emission fluxes is~~ Biomass burning emissions from Central Africa are of primary importance to simulate West African pollution (Giglio et al., 2006). This is achieved using the APIFLAME model (Turquety et al., 2013), which estimates aerosols and chemical species emissions produced by ~~vegetation fires~~ biomass burning. Since the incomplete combustion is both included in anthropogenic inventories (local urban burning) and ~~fires emissions inventories (biomass burning of forests)~~ forests biomass burning inventories, the simulation was designed to split these two parts.

Biogenic emissions are calculated using the MEGAN emissions scheme (Guenther et al., 2006). The mineral dust sources are obtained using ~~a the~~ GARLAP (Global Aeolian Roughness Lengths from ASCAT and PARASOL) new global soil and surface ~~datasets made from a dataset made from~~ satellite-derived aeolian roughness ~~length data lengths~~ with a 6 km spatial resolution ~~GARLAP (Global Aeolian Roughness Lengths from ASCAT and PARASOL) (Menut et al., 2013b), as detailed in~~ Mailler et al. (2016).

The top and lateral boundary conditions are driven by LMDZ-INCA for aerosols and chemical species (Folberth et al., 2006). The time step is set to 10 minutes for the physical processes and 5 minutes for the chemistry, which could change depending on the Courant-Friedrichs-Lewy condition. It is also possible to release gaseous or particulate atmospheric tracers, which is a powerful tool to analyze the pollution patterns.

Bessagnet et al. (2004) described the calculation of gaseous species in the MELCHIOR-2 (reduced) scheme and the aerosol scheme, which takes into account species such as sulphate, nitrate, ammonium, primary organic matter (POM) and elemental carbon (EC), secondary organic aerosols (SOA), sea salt, dust and water. All aerosols are represented using ten bins, from 40 nm to $40 \mu\text{m}$ in diameter. Their life cycle is fully represented with emission, transport, chemistry and deposition (wet and dry).

~~The top and lateral boundary conditions are driven by LMDZ-INCA for aerosols and chemical species (Folberth et al., 2006). It is also possible to release gaseous or particulate atmospheric tracers, which is a powerful tool to analyze the pollution patterns~~

Menut et al. (2016) have detailed and analyzed aerosol speciation and size distribution in the CHIMERE model during the summer 2013 over Europe and Africa using the AERONET network for AOD and EMEP network for PM concentrations. For

the AOD calculation, the aerosol optical scheme in the CHIMERE model considers mixed aerosols following the 'core-shell' hypothesis detailed in [Péré et al. \(2009\)](#) and evaluated in [Péré et al. \(2010\)](#).

In order to quantify the PM_{2.5} source apportionment, we assume that it is possible to split aerosols in different families depending on the sources because their chemical compositions are different: Mineral, Biogenic, Salt and Anthropogenic.

5 Given that anthropogenic and biomass burning aerosols have similar compositions, we have done two simulations with and without biomass burning emissions to split their contributions. The gas phase chemical scheme for SOA formation explained in [Bessagnet et al. \(2010\)](#) takes into account three anthropogenic and three biogenic hydrophilic species, three hydrophobic species with different saturations, and two surrogate compounds for the isoprene oxidation products.

10 The source apportionment has been determined for CO considering three main contributors (anthropogenic sources, biomass burning sources and long-range transport). Consequently, three simulations have been done: one without any emission source in the domain for the background concentration, one with the anthropogenic emission only, and a last one with the anthropogenic and biomass burning emissions.

3 Temporal variability from May to July 2006

In this section, we ~~first analyze and quantify~~ [analyze](#) the temporal variability of ~~the pollutants concentrations modeled in the urbanized areas along the Guinean Gulf coast~~ [precipitation, gas and aerosols](#) during the whole AMMA-SOP1 period ([Reidelsperger et al., 2006](#)). First, the precipitation regimes are ~~analyzed~~ [identified](#) using Hovmöller diagrams. Second, AERONET surface stations data are used to quantify the three-months variability of the Aerosol Optical Depth (AOD). Finally, the relative contribution ~~of several sources are quantified using the model~~ [to gases and aerosols from several sources is quantified using both airborne observations and modeling](#). The two last points focus on three locations: Cotonou (Benin), Djougou (Benin) and Niamey (Niger), which are representative of locations under ~~several influences (the combined influence of~~ [mineral dust, anthropogenic pollution and vegetation fires\)](#), [biogenic and biomass burning components](#).

3.1 Precipitations Patterns

During this period, the precipitation location and rate will play a crucial role ~~on for~~ [the modeled surface PM_{2.5} concentrations](#). As a validation for this variable, the methodology of [Flaounas et al. \(2010\)](#) is used: precipitation rates are averaged between 25 8.5°W and 8.5°E. Day-to-day variability is smoothed by applying a moving average of ± 2 days. Figure 2 is directly comparable to the [Flaounas et al. \(2010\)](#) study using the same period and averaged region. ~~Results show~~ [In May and June, observed and modeled precipitations occur mainly over the ocean \(below 5°N\). From late June on, the main precipitation areas move over the continent \(above 5°N\) and reach the Sahel \(at about 13°N\). Figure 2 shows](#) that the modeled precipitation spatial patterns are in good agreement with the two satellite observations (TRMM and GPCP) presented in their study [\(see Figure 3 of Flaounas et al. \(2010\)\)](#).

The WAM is ~~due to~~ [driven by](#) the sea surface temperature decreases ~~, which forms a cold tongue, over the Gulf of Guinea~~ and over the Sahara, a low thermal pressure system appears called the Saharan Heat Low ([Lafore et al., 2011](#)). The temperature

gradient between the sea and the Sahara allows the monsoon system to progress inland reaching the Sahara in July (Hall and Peyrill , 2006; Lavaysse et al., 2009). ~~We can notice on Figure 2 that the~~ The monsoon progression to the North is not linear. ~~Two jumps are observed due to the complex sea-land-atmosphere interactions constituted of two steps: the monsoon 'pre-onset' occurs (Figure 2). Two jumps are modeled at the~~ end of May ~~when the main precipitation area associated to the Inter~~
5 ~~Tropical Convergence Zone (ITCZ) located at 2 N moves to 5 N (Sultan and Janicot, 2000; Sultan and Janicot, 2003, 2003); and the monsoon 'onset' is another abrupt shift happening end of June when the main precipitation area moves from 5  to 10 N (Janicot et al., 2008). The precipitation and at the beginning of June. Precipitation~~ is associated with large scale squall-lines, creating Mesoscale Convective Systems (MCS) moving Westward (Hall and Peyrill , 2006).

The meteorological simulation reproduces the two changes of the main precipitation area ~~at the~~ that have been previously
10 identified from climatological averages: the 'pre-onset' (i.e. end of May), when the main precipitation area associated to the Inter Tropical Convergence Zone (ITCZ) located at the equator moves close to the coast (Sultan and Janicot, 2000; Sultan and Janicot, 2003
and the 'onset' (i.e. the 'pre-onset') and i.e. at the beginning of July (i.e. the 'onset'), when the main precipitation area reaches the Sahel (Janicot et al., 2008). For these dates, simulated ~~precipitations match very well AMMA observations which have shown that the 2006 monsoon onset date was the 10 July~~ precipitation matches very well with AMMA observations. In 2006,
15 the monsoon onset occurred on the 10 July with a 10-day delay compared to its climatological date, ~~i.e. which is~~ 24 June with a standard deviation of 8 days over the period 1968-2005 ~~(Janicot et al., 2008)~~ according to Janicot et al. (2008). Thus, three periods could be defined: before 'pre-onset' (in May), between 'pre-onset' and onset (in June), after onset (in July).

3.2 Meridional aerosols content

In our studied region, surface aerosol concentrations in the cities are affected by several contributions. In addition to local
20 emission, cities may be strongly impacted by biomass burning transported from ~~the Central Africa (Mari et al., 2007)~~ Central Africa (Mari et al., 2007) (Williams et al., 2010), or by mineral dust transported from Sahara (Flamant et al., 2009).

The modeled daytime Aerosol Optical Depth (AOD) and Angstr m exponent are compared to observations from the AERONET network (Holben et al., 1998), available at ~~(aeronet.gsfc.nasa.gov)~~. From the daily AERONET level-2 measurements AERONET-AOD ~~at 440nm and (at 440 nm) and the~~ Angstr m exponent ~~440-870~~ (440 nm - 870 nm), AERONET-AOD is
25 ~~calculated at 600nm (at 550 nm)~~ based on the Angstr m law. A spatial bilinear interpolation of the model outputs is performed at the station location.

Two AERONET stations are located close to the meridional transect studied (Figure 1): Banizoumbou (13.5 N, 2.1 E) in the suburb of Niamey in Niger, and Djougou in Benin (9.7 N, 1.6 E) North of the strongly urbanized areas around Cotonou.
~~Comparisons are~~ We compare a simulation made with and without biomass burning emission (with/without BB), presented in
30 Figure 3.

There are two important events of coarse particles recorded at both sites, associated with a low Angstr m exponent (*i.e.* Angstr m exponent lower than 0.5 as in Ogunjobi et al. (2008)) and AOD greater than 1, between 13-14 May and between 10-13 June. The model captures the magnitude of these large scale dust events. During the studied period, the events of coarse particles are well reproduced (high or moderate AOD are generally associated with a low Angstr m exponent). There is an

increase of the Angström exponent, *i.e.* fine particles over the period, which is well reproduced by the model. Frequent fine aerosol events (high Angström exponent) have been monitored corresponding to low or moderate AOD, which are partially captured by the model.

The addition of the biomass burning ~~emission~~emissions lead to an important plume of gas and aerosols reaching the Guinean ~~gulf~~Gulf in June. Modeled AOD with biomass burning emissions are well in the range ~~with biomass emission (bias is reduced)~~of the observations but the variability is not captured. ~~The Angström exponent is associated in May with~~In May, the aerosol content is mostly composed of coarse particles (Angström exponent about 0.2), in June ~~with of a~~ fine/coarse mixture of particles (about 0.5), in July ~~with a fine particles~~(of finer particles, especially at Djougou (Angström exponent about 0.8)). The model is able to reproduce this increase of the Angström exponent, which suggests an aerosol origin transition, from a period dominated by desert dust to a period of fine particles which could be local urban or/and biomass burning pollution from the South.

3.3 Meridional aerosols and gases concentrations

In this section, ~~firstly~~ the modeled CO and PM_{2.5} concentrations are compared to aircraft observations collected during the AMMA campaign. ~~Secondly~~(3.3.1). Then, the different ~~contribution~~contributions of the pollution sources ~~is~~are analyzed from the modeled concentrations at the three studied sites (3.3.2).

3.3.1 Airborne observations

~~Two flights made during a 'North-South land-atmosphere-ocean interaction' mission plans have been conducted over the Cotonou-Niamey meridional transect~~We are studying two flights conducted along a meridional transect between Cotonou and Niamey on 13 and 14 June 2006. These two days correspond to disturbed dynamics of the WAM due to 2006 as part of a 'North-South land-atmosphere-ocean interaction' survey mission. During these two days, the WAM dynamics over the area were perturbed by the presence of a MCS. It developed in the vicinity of the Jos plateau in the North of Nigeria over the Jos Plateau (Nigeria) around 16UTC, moving westward to the center of Ghana, which have already been described (e.g. (Flamant et al., 2009) and (Crume yrolle et al., 2011)). Moreover, the :00 UTC, reaching the Benin-Nigeria border at 20:00 UTC and moved southwestward across Benin overnight and into central Ghana, as already described in Flamant et al. (2009) and (Crume yrolle et al., 2011). The model reproduces the location of this MCS but earlier than in the observations, i.e. reaching the Benin-Nigeria border at 10:00 UTC (Figure 4). The MCS interacts with the dust layer coming from the Sahara (especially from the Bodele depression), changing the dust load and vertical distribution over Benin and Niger. Associated with subsidence in the wake of the MCS, there is a lowering of the dust layer height ~~(Flamant et al., 2007)~~(Flamant et al., 2009).

Modeled CO and PM_{2.5} concentrations are compared to aircraft measurements performed onboard the ATR-42 aircraft (with PCASP instrument for PM), which have been averaged at a 2-minute time step. The modeled values are interpolated along the aircraft trajectories, in time between the two closest modeled hourly outputs, and vertically between the two closest model vertical levels and horizontally with a bilinear interpolation. For the two flights (13 July in the morning from Niamey to Cotonou, and 14 July in the afternoon from Cotonou to Niamey), Table 1 presents modeled and observed mean spatial ~~value and range~~values and ranges of CO and PM_{2.5} concentrations in the PBL (altitude lower than 1000 m) over three regions: Coastal

region including Cotonou (6.3°N - 9.0°N), Sudano-Guinean region including Djougou (9.0°N - 11.0°N), Sudano-Sahelian region including Niamey (11.0°N - 13.5°N).

For CO concentration, on 13 June, there is no clear gradient over the three regions but rather a constant concentration of about 170 ppb. On 14 June, ~~a gradient is noticed~~ we can notice a gradient from the coast (200 ppb) to the Sahel (167 ppb).

5 For both days, the model ~~predict an opposite~~ predicts a gradient with the highest concentration over the Sahel. Over the coastal region, the observed CO concentration range is similar for the two flights (between 147 - 222 ppb), which is well in agreement with the modeled range (between 175 - 240 ppb). Over the Sudano-Guinean region, the observed range of variation is 161 - 182 ppb prior to the MCS (13 June), and it increases to 153 - 233 ppb after the MCS (14 June). The model is able to capture the larger range variability on 14 June ~~than on 13 June~~ (205 - 247 ppb compared ~~with to~~ 218 - 245 ppb on 13 June). Over
10 the Sudano-Sahelian region, the observed range variability of CO concentration is also larger on 14 June (146 - 200 ppb) than on 13 June (149 - 174 ppb). This behavior is not reproduced in modeled concentrations. There is an over-estimation of the modeled CO concentration (positive bias of ≈ 20 ppb) for 13 and 14 June.

For ~~the~~ PM_{2.5} concentration, a South-North gradient is expected ~~moving closer with the highest concentrations~~ close to the Sahara. There is a clear gradient in the observed PM_{2.5} concentration mean on 13 June ~~between the coastal region~~ (8 $\mu\text{g.m}^{-3}$ for the coastal region, -) and the Sudano-Guinean region (50 $\mu\text{g.m}^{-3}$ for the -), and almost the same concentration
15 in the Sudano-Guinean region, and the Sudano-Sahelian region (56 $\mu\text{g.m}^{-3}$ for the Sudano-Sahelian region). After the MCS, there is no clear gradient but rather the same concentration over the coastal and the Sudano-Guinean regions (39 $\mu\text{g.m}^{-3}$) ~~and a gap of concentration over~~. However, there is an important increase of the concentration moving to the Sahel (up to 92 $\mu\text{g.m}^{-3}$). The ~~ranges are~~ variability is increased over the three regions: 37 - 42 $\mu\text{g.m}^{-3}$ for the coastal region, 24 - 59 $\mu\text{g.m}^{-3}$
20 for the Sudano-Guinean region, 50 - 139 $\mu\text{g.m}^{-3}$ for the Sudano-Sahelian region. The modeled ranges match the observed ~~one ones~~ for both days. The model ~~reproduce~~ reproduces a South-North gradient on 13 June, which is well in agreement with the observations. On 14 June, the model ~~predict~~ predicts the concentration gap between the coastal and the Sudano-Guinean regions (from 43 to 82 $\mu\text{g.m}^{-3}$), while it was observed between the Sudano-Guinean and the Sahelian regions.

~~The 13 and 14 June 2006 correspond to disturbed~~ These two days correspond to disturbed meteorological conditions, which
25 may not be representative of the typical average concentrations. The model-observation comparison ~~suggest~~ suggests that the MCS ~~is not well reproduced~~ occurs later in the observation, which could in turn induce a ~~not realistic~~ unrealistic modeled pollution plume (for instance a biomass burning plume) over the Sudano-Sahelian region and the Sahel. Nevertheless, ~~there is a over-estimation of the modeled CO concentration (positive bias of ≈ 20 ppb) for these two days~~ the order of magnitude of the CO and PM_{2.5} concentrations are good in agreement with observations.

30 3.3.2 Monthly modeled pollution sources apportionment

In order to analyze the source apportionment, we consider that the CO mixing ratio is due to three major sources: background, anthropogenic and ~~fires, and biomass burning, and that~~ the PM_{2.5} mass concentration comes from five major types of pollution source: anthropogenic, ~~fires~~ biomass burning, mineral dust, biogenic and sea salt (we assume that PM_{2.5} background concentration is negligible). ~~For the whole period and for each month of the simulation, the~~ The relative percentage of each source is

presented for CO in Table 2 and for PM_{2.5} Table 3 at the three studied locations: Cotonou, Djougou and Niamey, for the whole period and for each month of the simulation.

For the three sites, the average concentrations of surface CO increase during the whole period. The mean concentrations are very close for the three sites: 221 ppb in Cotonou, 227 ppb in Djougou, and 212 ppb in Niamey. There is a clear increase of ~~the~~ CO from May (157 - 180 ppb) to July (267 - 280 ppb). This increase is due to the ~~vegetation-fire-biomass burning~~ sources from May (3 - 10 %) to July (40 - 49 %), while the anthropogenic and background concentrations are stable during the whole period and for ~~the three-all~~ sites. It seems that the CO overestimation noticed in the previous section is linked with an overestimation of ~~vegetation-fire-biomass burning~~ emissions.

~~Considering~~ PM_{2.5} concentrations ~~, there is on average over the whole period display~~ a South-North gradient of concentrations (30 $\mu\text{g.m}^{-3}$ in Cotonou, 38 $\mu\text{g.m}^{-3}$ in Djougou, 54 $\mu\text{g.m}^{-3}$ in Niamey) on average over the whole period, consistent with the gradient of ~~the~~ dust contribution (15 % in Cotonou, 35 % in Djougou, 67 % in Niamey). From May to July and for ~~the three-all~~ sites, the mineral dust contribution is in constant decrease. On the other hand, the ~~vegetation-fires-biomass burning~~ contribution increases (3 to 19 $\mu\text{g.m}^{-3}$ in Cotonou, 1 to 17 $\mu\text{g.m}^{-3}$ in Djougou, 0.6 to 11 $\mu\text{g.m}^{-3}$ in Niamey), which ~~could seems to~~ be overestimated as for CO concentration. PM_{2.5} concentrations are dominated by natural sources. ~~Nevertheless~~ ~~anthropogenic-Anthropogenic~~ PM_{2.5} concentrations range ~~between-from~~ 3 to 5 $\mu\text{g.m}^{-3}$, which is about 10 % for the whole period and for the three sites.

In Cotonou, the average ~~concentrations-concentration~~ of surface PM_{2.5} increases during the whole period, from 23 to 37 $\mu\text{g.m}^{-3}$. This mainly corresponds to the arrival of ~~vegetation-emissions-biomass burning emission~~ products, transported from Central Africa to the Guinean Gulf, with an increase from 11 to 52 % from May to July. On the contrary, the mineral dust contribution decreases during the period, from 38 to 5 %. The sea salt contribution increases from 3 to 6 ppb. During the three months, the anthropogenic and biogenic contributions remain ~~stables-stable~~ at about 4 ~~ppb- $\mu\text{g.m}^{-3}$~~ and 6 ~~ppb- $\mu\text{g.m}^{-3}$~~ respectively.

In Djougou, the same behavior is observed but with some changes in the absolute values. The relative contribution of mineral dust decreases from 57 % to 14 %, while the ~~fire-biomass burning~~ contribution increases from 3 to 47 %. The anthropogenic contribution is slightly higher in June at about 5 ~~ppb- $\mu\text{g.m}^{-3}$~~ .

In Niamey, the dust contribution is important for the three months. It decreases by a factor 4, from 61 to 15 $\mu\text{g.m}^{-3}$, ~~econsistently-consistent~~ with observation of PM₁₀ in Banizoumbou in Niger (Marticorena et al., 2010), which is probably due to the reduction of local emission linked with the increase of vegetation cover. The relative contribution of anthropogenic pollution is slightly higher in June at about 5 ~~ppb- $\mu\text{g.m}^{-3}$~~ .

For CO or PM_{2.5} concentrations, the anthropogenic ~~contribution-is-always-important-in-emissions~~ contribute significantly to the total budget (≈ 30 % for CO and ≈ 10 % for PM_{2.5}). It is therefore important to better understand the daily variability of anthropogenic ~~pollutants-pollutant~~ transport.

4 Focus on anthropogenic pollutants from Cotonou to Niamey

This section focuses on ~~anthropogenic pollution~~the horizontal variability and vertical structure of anthropogenic pollution. Only the contribution of anthropogenic sources is considered in $\text{PM}_{2.5}$ and CO concentrations, from now on referred to as anth- $\text{PM}_{2.5}$ and anth-CO.

5 4.1 Time-latitude variability at the surface

4.1.1 CO and $\text{PM}_{2.5}$ concentrations

The Cotonou-Niamey meridional transect includes the two specific cities extensively studied in the framework of the AMMA program: a coastal megacity (Cotonou in Benin) and a Sahelian city (Niamey in Niger). To highlight the latitudinal regional transport, modeled concentrations are presented with the same methodology as in the previous section with Hovmöller diagrams, corresponding to time-latitude average of variables (data are smoothed with a 5-day moving average, *i.e.* ± 2 days).

Results are presented in Figure 5 for anth-CO and anth- $\text{PM}_{2.5}$. For the two species, meteorological parameters are superimposed to-on the concentrations. ~~The precipitation~~Precipitation rate contours are defined for events with more than 10 mm/day over the Cotonou-Niamey transect. These are similar but not equivalent patterns to those presented in section 3.1 averaged over the entire West Africa.

15 The Inter-Tropical Discontinuity (ITD) is the limit between the northward monsoon wind and the southward Harmattan wind (Flamant et al., 2007; Karam et al., 2009). The ITD could be defined as the isocontour of relative humidity (RH) equal to 20 %. We can notice that the location of the ITD ~~marks-associated with~~ a sharp gradient in surface anthropogenic concentrations, with a decrease going further North from 100 to 20 ppb for CO, and from $5 \mu\text{g.m}^{-3}$ to $2 \mu\text{g.m}^{-3}$ for $\text{PM}_{2.5}$.

For anth-CO surface concentrations, high concentrations are continuously ~~noticed-during-the-whole-period~~modeled from
20 the beginning of May to late June at the coast where Cotonou is located, about 100 ppb around $\phi = 6.3^\circ\text{N}$. Over the Guinean ~~gulf~~Gulf, the concentration is low between 20 and 50 ppb. The second area with high anth-CO values corresponds to the Sudano-Sahelian region, where concentration vary between 60 and 100 ppb around $\phi = 12^\circ\text{N}$. Whereas high concentrations of anth-CO at the coast ~~is-are~~ clearly related to local emissions, the high concentrations over the Sahel ~~should-could~~ be either due to transport, or local emissions. Over the studied domain, anth-CO surface concentrations ~~evolves-evolve~~ between 20 and 120 ppb.

25 There are ~~in-May-and-in-June~~ some high modeled surface concentrations in May and in June when rain occurs, such as around 11 June. In July, the variability is mostly consistent with precipitation rates after the onset, ~~which-suggest-that-surface-versus-vertical-distribution-has-changed~~suggesting modifications of transport and deposition patterns by the convection associated with large scale precipitation. ~~The precipitation~~Precipitation variability can thus explain only a part of the CO variability. It is necessary to also investigate the large-scale wind speed and direction.

30 The same behavior is observed for the surface concentrations of ~~PM~~anth- $\text{PM}_{2.5}$. The week to week variability is ~~more important~~. ~~This-increase-greater-than-for-anth-CO~~, which is probably due to the longer ~~CO-lifetime~~lifetime of CO compared with that of PM (being less chemically active and ~~without-settling~~), ~~the-CO-concentrations-are-less-prone-to-settling~~. CO is more homogeneously mixed than PM in a large latitudinal area spanning from the coast to ~~more-latitudes~~higher than 16°up

to the North. The temporal variability of surface $\text{PM}_{\text{anth-PM}_{2.5}}$ exhibits a ~~frequency close to 2-week~~ periodicity close to two weeks: during the whole modeled period, five higher concentration periods are observed from the coast to $\phi \approx 16^\circ\text{N}$. In addition in these latitudinal ~~plumes patterns~~, local minima are modeled, for instance the 20 June at $\phi \approx 13^\circ\text{N}$. At $\phi = 12^\circ\text{N}$, there is an area of high concentration ~~;~~ which is present over the whole period. This may be related to vertical transport and will be quantified in the next sections. The results showing similarities for both two pollutants in terms of time-latitude variability, the next sections will refine the ~~analyzes only for PM~~ analysis only for anth-PM_{2.5}.

4.1.2 Synoptic wind and pollution

This section aims at analyzing the anth-PM_{2.5} concentration temporal ~~frequency-variability~~ through the surface wind speed and direction. The previous section has shown that low pollution ~~levels are~~ concentration is not always associated with precipitations. Results are presented in the same way using Hovmöller diagrams ~~on Figure 6~~ (Figure 6). For each figure, colored isocontours are superimposed corresponding to surface anth-PM_{2.5} of 4 and 5 $\mu\text{g.m}^{-3}$.

For the surface wind speed, the lowest values are modeled along the coast during the whole period. The wind speed variability is weak from the coast to the Sahel. Periods of low wind speed are coincident with the highest values of surface $\text{PM}_{\text{anth-PM}_{2.5}}$. At the end of the period, ~~when precipitation occurs inland and anth-PM_{2.5} is low~~, the meteorological situation changes ~~and the wind speed increases~~ suddenly over the ocean showing the cold tongue arrival ~~as previously described by Meynadier et al. (2016); when there are precipitations inland and low anthropogenic pollution levels located at the Equator, which is associated with increased wind speed between the Equator and the coast, as detailed by Meynadier et al. (2016).~~

Regarding the ~~precipitations~~ precipitation occurrences discussed in the previous section, the high surface anth-PM_{2.5} concentrations modeled around $\phi = 12^\circ\text{N}$ are due to a combination of low wind speed and low precipitation rates. These meteorological conditions are representative of stagnation, which accumulate pollutants in the lowest layers of the troposphere.

For the surface wind direction, the main wind direction near the coast is the South-West quarter during the whole period. There is no obvious link between wind direction changes and PM_{2.5} highest values over the Cotonou-Niamey meridional transect.

The large scale variability of meteorological variables (precipitation and wind speed) controls the period of high anthropogenic pollution from the coast to the Sahel. However, it does not explain if the high concentration over the Sahel are linked with local emissions or/and with pollutants transport from the coast.

4.2 Monthly mean vertical structure

4.2.1 Anthropogenic pollution

We now focus on the vertical structure of the lower troposphere from the surface to 4 km altitude in order to understand ~~what is responsible for hte causes of~~ the high anth-PM_{2.5} concentration over the Sahel. Monthly averages of anth-PM_{2.5} concentration are analyzed together with wind ~~circulations~~ circulation (monthly averages correspond to consistent meteorological periods, c.f. Section 3.1). In Figure 7, the modeled concentrations are spatially averaged over the Cotonou-Niamey meridional transect.

Three isocontours (3, 4 and 5 $\mu\text{g.m}^{-3}$) are used to follow the anthropogenic pollution patterns. Results are presented at 00 UTC when the NLLJ is ~~established (on the contrary, well established~~ (during the day, the pollution is more mixed in the PBL by dry convection).

For the three months, the meridional wind is lower at the surface than in the boundary layer from the coast to $\approx 9^\circ\text{N}$, highlighting the well established NLLJ. Above the northward monsoon flux, there is the SAL associated with southward winds. The highest southward wind speed in the core of the SAL between 11 and 16°N in latitude and 2 to 4.5 km in altitude is the African Easterly Jet (AEJ).

Regarding the wind, two atmospheric cells are ~~noticed on Figure 7 modeled~~ during the three months (Figure 7). There is a large cell going northward at the surface within the monsoon flow, and going backward toward the South with the SAL (or AEJ), located at ≈ 2 km altitude, ~~and between the coast and $\approx 16^\circ\text{N}$~~ . There is also a small cell turning in the same direction (~~clockwise anti-clockwise~~) at ≈ 2 km altitude, with the downdraft at 6°N and the updraft at 7°N . In May and June, the small cell is included in the large cell, while in July, they are disconnected. ~~These two cells seem to interact with the anthropogenic pollution because the anth-PM_{2.5} isocontours shape appear to be driven by the wind patterns.~~

Regarding anth-PM_{2.5} concentration, these two atmospheric cells seem to interact with the anthropogenic pollution because the anth-PM_{2.5} isocontours shape appear to be driven by the wind patterns. The large atmospheric cell induces a recirculation of the modeled anthropogenic plume, ranging from $\phi = 6$ to 18°N in latitude and 0.5 to 3 km in altitude (anth-PM_{2.5} isocontour of 3 $\mu\text{g.m}^{-3}$). ~~We can notice that the recirculation center~~ The center of this cell is located at $\phi \approx 14^\circ\text{N}$ during the three months studied. In May, an important part of the pollution from the coast is transported in altitude within the NLLJ above the PBL (displayed by the anth-PM_{2.5} isocontour of 4 $\mu\text{g.m}^{-3}$). In June, there is high concentration in altitude over the Sahel (displayed by the anth-PM_{2.5} isocontour of 5 $\mu\text{g.m}^{-3}$), which suggests that the atmospheric cell concentrates pollutants. Note that in July, ~~the lowest latitude of the anthropogenic plume is moved northward, starting at $\approx 10^\circ\text{N}$, and less connected with the coast~~ high anth-PM_{2.5} concentration are only modeled along the coast and close to the surface.

Air masses transport anthropogenic pollutants from the coast to the Sahel. High surface concentrations of anth-PM_{2.5} are modeled at the latitude of the coastal urbanized areas ($\phi = 6.3^\circ\text{N}$), leading to a plume to the North within the NLLJ and concentrating pollutants over the Sahel.

4.2.2 Coastal versus Sahelian pollutants meridional transport

A tracer experiment has been set-up to analyze if the main contributors to the Sahelian maximum are emitted locally or remotely at the coast. Gaseous tracers are released at the two major cities of the meridional transect (~~without any sink~~): ~~Cotonou (Benin)~~ and Niamey (~~Cotonou in Benin and Niamey in Niger~~). The ~~tracers~~ tracer experiment uses arbitrary units and considers the same quantity of tracers emitted in each town. The tracers are constantly released from the 1 to 30 June. The emission altitude occurs in the PBL (0 - ~~500~~ 200 m) from the 1 June to 30 June. Results are presented ~~in Figure 8~~ averaged during the ten last days at 00 UTC ~~considering as in the previous section. We consider either~~ only coastal emissions or only Sahelian emissions in order to observe where air recirculation may concentrate the pollutants (Figure 8).

Tracers emitted at the coast indicate that there is ~~a contribution~~ an important transport of coastal pollutants ~~over the Sahel~~. ~~The ratio of Sahelian tracers concentration and coastal tracers concentration toward the North in the PBL. On the other hand,~~ there is no significant transport of tracers emitted in the Sahel is between 10 % and toward the coast. In Niamey, Cotonou tracer concentration is about 9% (of the 1 %; i.e. with coastal emission 10 to 100 times higher, the anthropogenic coastal
5 pollution could be equivalent to the anthropogenic Sahelian pollution over the Sahel a.u. isocontour presented in Figure 8-a), while in Cotonou, Niamey tracer concentration is about 0.03% (of the 1 a.u. isocontour presented in Figure 8-b). In the HTAP anthropogenic inventories (presented in Figure 1), the anth-PM_{2.5} (respectively anth-CO) is ~~at Niamey~~ at Niamey ≈ 103 (735) $\text{kg.km}^{-2}.\text{day}^{-1}$ ~~and at Cotonou~~ in Niamey and ≈ 438 (7707) $\text{kg.km}^{-2}.\text{day}^{-1}$ in Cotonou. Therefore, an important part of the pollution over the Sahel has been emitted at the coast ~~;, which and it~~ contributes to a maximum of anthropogenic pollution
10 in June over the Sahel. In conclusion, the high concentration ~~in altitude~~ over the Sahel ~~are due to atmospheric cells, which~~ concentrate is due to the existence of a meridional atmospheric cell, which acts at accumulating pollutants emitted locally and remotely at the coast.

5 Impact of coastal dynamics on anthropogenic pollution

In order to better characterize ~~the~~ coastal pollution, ~~anthropogenic PM~~ anth-PM_{2.5} for the period of 8 to 15 June 2006 are now
15 described at hourly temporal resolution. This week includes a large variability of low to high surface concentrations.

5.1 Surface hourly pollution variability

The ~~surface hourly anthropogenic PM~~ hourly surface anth-PM_{2.5} concentrations are shown ~~on in~~ Figure 9 over the Cotonou meridional transect ~~;. The highest temporal resolution shows the same variability as described in Figure 5 with the with~~ Hovmöller diagrams. The beginning of the week associated with lower concentrations ~~-.
20 , as already described in Figure 5.~~ For most days, the highest ~~surface~~ concentrations are modeled between 18 UTC and 00 UTC from the coast to 8°N. This coincides with the lowest boundary layer height, which concentrates urban emissions (i.e waste burning and traffic) in a thin layer (not shown). ~~It seems that urban plumes start from the coastline, corresponding to the city, at the sunset (18 UTC) and derives to the North in the next few hours.~~

At the coast, anth-PM_{2.5} concentration decreases at night (between 00 UTC and 06 UTC) and ~~;, increases again~~ in the morning (around 06 UTC) ~~;, concentration increases again at the surface when the convection and NLLJ are weak, which follows traffic emissions. This feature follows traffic emissions, which are included in the anthropogenic emission inventories. It seems that urban plumes start from the coastline at sunset (18 UTC) and are transported to the North in the following hours.~~

There is a transition from low to high level concentration of anthropogenic pollution from ~~the~~ 8 to 12 June. Anthropogenic pollution is modeled over the sea from 10 to 11 June. It is interesting to note ~~on the 11-12 June night that high concentrations~~ are modeled during the day when there is precipitation inland that precipitation occurs inland on 11 June (between 18 UTC and
30 00 UTC), then high modeled concentrations persist during the night of 11-12 June. This precipitation event reflects a change

in the wind patterns, which induces a change in the transport of pollutants~~over the sea (with~~, leading to surface concentrations up to $3.8 \mu\text{g.m}^{-3}$ in Cotonou.

5.2 Contribution of other cities at Cotonou

At the coast, the wind direction comes from the sector S-SW but there are diurnal variations ~~,~~ which could affect the air pollution along the coastline. In order to distinguish ~~pollutants~~ pollutant transport from the different coastal megacities, a tracer experiment has been ~~set-up~~ set up. The tracers are constantly released in the lowest model layers ranging from surface to 500 m above sea level. This altitude corresponds to emission below or within the NLLJ. Three point sources have been defined: Accra in Ghana (5.6°N, 0.2°W), Lome in Togo (6.2°N, 1.2°E) and Cotonou in Benin (6.4°N, 2.4°E). The results are presented over the Cotonou meridional transect (Figure 10). We aim at evaluating the impact of the Cotonou local emissions versus emissions from distant areas transported toward Cotonou. The emission (in arbitrary unit) has the same magnitude in each city without any daily variation.

As expected, the surface concentrations of Cotonou due to local emission only are the highest at the coast. The diurnal cycle of ~~pollutants~~ pollutant transport appears clearly with the highest concentrations exported at the beginning of the night (18 UTC), when the boundary layer height decreases quickly and when the establishment of the NLLJ occurs. Up to 9°N, high tracers concentrations are transported from Cotonou far from the point source. The Cotonou plume always transports tracers up to 7°N; for some days, these plumes may reach the latitude of 9°N during the night between 18 UTC and 06 UTC.

At Cotonou, the modeled tracers concentration released from Lome or Accra are logically lower because the source points are not in the Cotonou meridional transect~~studied~~. The same kind of northward transport is observed but pollutants transport from Accra and Lome reach Cotonou in the morning between 06 UTC and 12 UTC for the Lome plume, and in the afternoon between 12 UTC and 18 UTC for the Accra plume. This result is consistent with a transport speed between 10 and 20 km.hour⁻¹ (the Lome-Cotonou distance is about 150 km, and Accra-Cotonou about 300 km) ~~. Moreover, there is probably a diurnal variation of the wind direction, coming and synoptic wind direction from the sector S-SW during the day and SW-W at night because of the land/sea breeze, which carry more efficiently pollutants emitted during the night toward Cotonou.~~

S-W. In arbitrary unit and with the same emission at the three cities, ~~the concentrations modeled at latitude modeled~~ concentrations between 7°N and 8°N are similar for the Lome and Cotonou plumes, and ~~in a lower extent lower~~ for the Accra plume. ~~This means that the urbanized areas West from Cotonou (Lome or Accra) contribute as much as Cotonou to the anthropogenic pollution at those locations (when considering the same emission).~~

The comparison between the three plumes shows a specific behavior during 10-12 June as the Cotonou pollution is not exported to the North:

- On 10 June, the Lome plume is clearly exported over the sea and very high concentrations are noticed over Cotonou. The same behavior is observed for the Accra plume with lower concentration because this location is further from Cotonou. Indeed, the Lome and Accra plumes reach Cotonou after being transported over the sea, which suggests that pollutants at the three cities have been transported Eastward, leading to plumes ~~overlaying~~ mixing at the Cotonou location.

- On 11 June, there are still high concentrations over Cotonou due to the Accra plume probably driven by the same meteorological conditions, but it does not affect the Lome plume ~~does not have a specific behavior~~. This suggests a perturbation affecting especially Accra.
- ~~The On~~ 12 June ~~corresponds to the most~~, there is an important transport of Cotonou ~~emission~~ pollution to the North. At the same time, this is the only day when Lome and Accra plumes do not reach Cotonou, as they are shifted to the North at 7°N when crossing the Cotonou meridional transect.

All these results suggest a fast change of the meteorological situation, leading to air pollution. In the next section, the specificity of the vertical wind structure during this period will be studied in detail.

6 Disturbed atmospheric dynamics and pollution transport

- 10 In this section the analysis is refined to two periods of two days on 8-9 and 11-12 June ~~2006~~. 2006 in the Cotonou area. The first corresponds to ~~non-perturbated non-perturbed~~ monsoon flow situation leading to low anthropogenic pollution, the second corresponds to a ~~disturbed perturbed~~ situation leading to high anthropogenic pollution.

6.1 Evolution of the vertical structure

- 15 In order to focus on the day/night transport from the coast to the North (described in section 5.1) and the changes in dynamical regimes during this period (described in section 5.2), results are presented as vertical slices in Figure 11, averaged along the Cotonou meridional transect. The tracers concentrations, emitted separately at Lome and Cotonou, are presented as isocontours of threshold values: the emissions being arbitrary, the modeled concentrations are also arbitrary. But the same threshold is used for the two emissions locations, thus concentration magnitudes are comparable. The wind vectors (meridional/vertical components) are superimposed on the figures to highlight the vertical cells. The meridional wind is also presented as color shading for the NLLJ intensity.

- 20 The first period ~~-(8 June at 23 UTC and 9 June at 11 UTC-)~~ corresponds to a classical monsoon case, often observed and described in the literature (Abdou et al., 2010; Lothon et al., 2008). At night, surface pollutants are concentrated in a shallow layer (less than 200m), corresponding to nocturnal surface layer and to the lowest part of the NLLJ (represented by the 'dark blue' shaded area in Figure 11). The Cotonou and Lome plumes are mixed. During the day, the convection induces ~~more mixing~~ over land than over sea, where the boundary layer reaches 1500 m mixing in the boundary layer, which reaches 1500 m at 11 UTC over the continent. The Lome plume does not reach the coast, but it crosses the Cotonou meridional transect ~~more further~~ to the North >6.5(≈ 7°N).

- 30 On 8-9 June, an updraft-downdraft convective cell is clearly observed during the day and at night, with ascendent wind at 7°N and subsident wind at 6.3°N (the Cotonou site latitude). This circulation has already been observed for the whole studied period in section 4.2.1. This is not a modeled land-sea breeze because it turns in the same direction day and night. Land-sea breezes have not been explicitly modeled because of the too coarse resolution (about 20 km).

The second period ~~;~~(11 June at 23 UTC and 12 June at 11 UTC~~;~~) corresponds to a disturbed case compared to what is usually observed in this region and for this month~~(for instance 8-9 June)~~. Indeed, for ~~the~~11 June at 23 UTC, the NLLJ is not present near the coast and the wind is weak from the coast to 8°N. The modeled nocturnal PBL height is very low (less than ~~50m~~50 m). The Lome plume is not present over Cotonou. On 12 June at 11 UTC, air subsidence is modeled from 7°N to 10°N. The isocontours of concentrations due to emissions in Lome and Cotonou are at the same latitude, corresponding to an iso-latitudinal transport, along the coast. Compared to ~~the~~8-9 June, there is no coastal cell located over the emission region. ~~But a~~A larger cell is modeled, with high meridional wind speed (up to 4 m.s⁻¹). The subsidence, located at $\phi > 7^\circ\text{N}$, imports upper air masses from the free troposphere and blocks the northward transport of the coastal pollutants.

6.2 Specificity of 11-12 June 2006

In this last ~~section~~analysis, we focus on the 11-12 June to understand which meteorological conditions have led to an important modeled anthropogenic PM_{2.5} event at Cotonou. Schwendike et al. (2010) have shown that a large MCS has occurred over Ghana due to convective instabilities at the border of Togo, Ghana and Burkina Faso. Some spots of convection ('Pop corn' convection) over a large region including Cotonou has been identified on 11 June. An isolated convective cell lasting a few hours coming from South-East and ~~going~~moving North-West ~~have~~has crossed the coastline over Cotonou at around 18 UTC (~~Figure ??~~Figure 12), which is well in agreement with the modeled location (Figure 13). When precipitation is inland between 19 UTC and 23 UTC(~~Figure 13 - top~~), the wind speed is null over the coast because the monsoon flux is blocked (Figure 13 - top). During these specific meteorological conditions, the high anth-PM_{2.5} surface concentrations are thus due to an accumulation of pollution during a few hours (from 19 to 23 UTC).

The same tracer experiment as described in ~~the previous sections (described in~~section 5.2 ~~)~~ is used to ~~test our hypothesis~~aboutconfirm the accumulation of pollutants and to distinguished plumes of the different cities. Gaseous tracers are released with the same emission at four cities: Accra (Ghana), Lome (Togo), Cotonou (Benin) and Lagos in Nigeria has been added (6.5°N,3.4°E) .

We can notice (~~on Figure 13 -bottom~~) that the pollution emitted at the different cities West from Cotonou is mixed at $\phi = 7^\circ\text{N}$ on 11 June at 19 UTC (Figure 13 -bottom). Six hours later, only the Cotonou plumes is responsible for the high anth-PM_{2.5}, which confirms pollutants accumulation because it has been blocked by the down-draft of the precipitation system during six hours.

This result demonstrates that during the monsoon period, specific meteorological conditions could lead to high pollution in the Guinean coast megacities, although most of the time pollution emitted along the coastline are quickly transported to the North.

7 Conclusions

~~The~~West African pollution ~~has been~~was studied using both models and observations during May, June and July 2006. This corresponds to the beginning of the ~~WAM and~~West African monsoon and it includes the AMMA campaign observational

period. The focus ~~is~~was on urbanized areas ~~,~~located along the Guinean Gulf coast and known as large gas and aerosol emitters. In addition to these anthropogenic emissions, the coast is often under the influence of long-range transport of mineral dust and ~~vegetation fires~~biomass burning emissions. The analyses are performed for CO and PM_{2.5} over a large domain to include all sources: Central Africa for biomass burning, Sahel and Sahara for mineral dust and a large part of the Guinea Gulf for sea salt.

The first analysis was devoted to estimate the relative contribution of each source during the three months in Cotonou (Benin), Djougou (Benin) and Niamey (Niger). It was shown that the surface concentrations of PM_{2.5} constantly increase during the period. The mineral dust ~~dust~~ relative contribution remains low close to the coast, showing that in monthly average, pollution during this period is not dominated by mineral dust transport events. On the other hand, the ~~vegetation fires~~biomass burning emissions increase from May to July. The anthropogenic part is stable during the whole period for the three studied sites at $\approx 50\%$ for CO and $\approx 15\%$ for PM_{2.5}.

The second part of the study ~~was focused on~~analyzed the anthropogenic contribution ~~of~~to CO and PM_{2.5} along a Cotonou-Niamey meridional transect. ~~A transport of these pollutants~~These pollutants are transported from the coast to the north ~~has been demonstrated up to as far as~~ the Sahel (13°N). The Northward limit of the transport corresponds to the Inter Tropical Discontinuity. It was also shown that there are alternating periods of high/low concentration from Cotonou to Niamey with a weekly frequency. To understand this variability, meteorological variables ~~have been~~were investigated. The highest surface pollutants concentrations occurred when there is no precipitation and low wind speed.

In order to better understand the meridional transport and the occurrence of high ~~pollutants~~pollutant concentrations over the Sahel ($\approx 13^\circ\text{N}$), monthly averages of vertical wind structure were analyzed. From May to June, a large atmospheric cell going from the coast to the Sahel remains present and it has been identified as responsible for ~~the~~the pollutant accumulation over the Sahel ~~of pollutants~~ emitted locally and remotely at the coast.

A focus ~~has been done~~was put on coastal dynamics and pollution transport during a restricted period, from 8 to 15 June 2006, ~~including which included~~ high and low ~~levels~~concentrations of anthropogenic pollution. To isolate the coastal dynamics impacts on several ~~cities plumes from~~city plumes along the coastline, a tracer experiment was designed with emissions at Accra (Ghana), Lome (Togo) and Cotonou (Benin). The tracer concentrations confirm that, in Cotonou, the modeled concentrations are ~~both due to~~due to both local and remote emissions. A meridional transport of the anthropogenic pollution from the coast to the North has been highlighted at night linked with the Nocturnal Low Level Jet close to the coast.

Finally, two contrasted anthropogenic pollution situations were ~~detailed~~analyzed in detail. The first situation (8-9 June) corresponds to low anthropogenic pollution during a 'typical' case of monsoon dynamics, while the second situation (11-12 June) corresponds to a disturbed meteorological situation due to a ~~MCS~~During the convective system. During 11-12 June, ~~it was shown that~~ air subsidence is modeled at latitude 7°N, which imports ~~clean~~ upper air masses from the free troposphere, limiting the northward transport of the coastal pollutants. ~~The main results of this article will be compared to~~

Concerning air quality and climate policy development, we showed that the export of anthropogenic pollutant from the Guinean coast toward the North could lead to cross boundary pollution plumes. This result will be confirmed by comparison

to the 2016 DACCIIWA campaign observations in order to ~~confirm and refine your conclusions~~ propose strategy to reduce atmospheric pollution in West Africa.

Acknowledgements. The research leading to these results has received funding from the European Union 7th Framework Programme (FP7/2007-2013) under Grant Agreement no. 603502 (EU project DACCIIWA: Dynamics-aerosol-chemistry-cloud interactions in West Africa). This work has been supported by the African Monsoon Multidisciplinary Analysis (AMMA) project. Based on a French initiative, AMMA was built by an international scientific group and is currently funded by a large number of agencies, especially from France, UK, USA and various African countries. The authors wish to thank the SAFIRE (Service des Avions Français Instruments pour la Recherche en Environnement) for preparing and delivering the research aircrafts (ATR-42). We thank the Philippe Goloub and Didier Tanre for their effort in establishing and maintaining AERONET sites in Djougou (Benin) and in Banizoumbou (Niger).

References

- Abdou, K., Parker, D. J., Brooks, B., Kalthoff, N., and Lebel, T.: The diurnal cycle of lower boundary-layer wind in the West African Monsoon, *Quarterly Journal of the Royal Meteorological Society*, 136, 66–76, doi:10.1002/qj.536, 2010.
- Akeredolu, F.: Atmospheric environment problems in Nigeria. An overview, *Atmospheric Environment*, 23, 783–792, 1989.
- 5 Ancellet, G., Orlandi, E., Real, E., Law, K. S., Schlager, H., Fierli, F., Nielsen, J. K., Thouret, V., and Mari, C.: Tropospheric ozone production related to West African city emissions during the 2006 wet season AMMA campaign, *Atmospheric Chemistry and Physics*, 11, 6349–6366, doi:10.5194/acp-11-6349-2011, 2011.
- Assamoi, E.-M. and Lioussé, C.: A new inventory for two-wheel vehicle emissions in West Africa for 2002, *Atmospheric Environment*, 44, 3985–3996, doi:10.1016/j.atmosenv.2010.06.048, 2010.
- 10 Asuoha, A. N. and Osu, C. I.: Seasonal variation of meteorological factors on air parameters and the impact of gas flaring on air quality of some cities in Niger Delta (Ibendo and its environs), *African Journal of Environmental Science and Technology*, 9, 218–227, doi:10.5897/AJEST2015.1867, 2015.
- Baklanov, A., Molina, L. T., and Gauss, M.: Megacities, air quality and climate, *Atmospheric Environment*, 126, 235–249, doi:10.1016/j.atmosenv.2015.11.059, 2016.
- 15 Baumbach, G., Vogt, U., Hein, K. R. G., Oluwole, a. F., Ogunsola, O. J., Olaniyi, H. B., and Akeredolu, F. a.: Air pollution in a large tropical city with a high traffic density - Results of measurements in Lagos, Nigeria, *Science of the Total Environment*, 169, 25–31, doi:10.1016/0048-9697(95)04629-F, 1995.
- Bessagnet, B., Hodzic, a., Vautard, R., Beekmann, M., Cheinet, S., Honoré, C., Lioussé, C., and Rouil, L.: Aerosol modeling with CHIMERE - Preliminary evaluation at the continental scale, *Atmospheric Environment*, 38, 2803–2817, doi:10.1016/j.atmosenv.2004.02.034, 2004.
- 20 Bessagnet, B., Seigneur, C., and Menut, L.: Impact of dry deposition of semi-volatile organic compounds on secondary organic aerosols, *Atmospheric Environment*, 44, 1781–1787, doi:10.1016/j.atmosenv.2010.01.027, 2010.
- Boman, J., Lindén, J., Thorsson, S., Holmer, B., and Eliasson, I.: A tentative study of urban and suburban fine particles (PM_{2.5}) collected in Ouagadougou, Burkina Faso, *X-Ray Spectrometry*, 38, 354–362, doi:10.1002/xrs.1173, 2009.
- Crétat, J. and Pohl, B.: How Physical Parameterizations Can Modulate Internal Variability in a Regional Climate Model, doi:10.1175/JAS-D-11-0109.1, 2012.
- 25 Crumeyrolle, S., Tulet, P., Gomes, L., Garcia-Carreras, L., Flamant, C., Parker, D. J., Matsuki, A., Formenti, P., and Schwarzenboeck, A.: Transport of dust particles from the Bodélé region to the monsoon layer - AMMA case study of the 9-14 June 2006 period, *Atmospheric Chemistry and Physics*, 11, 479–494, doi:10.5194/acp-11-479-2011, 2011.
- Cuesta, J., Marsham, J. H., Parker, D. J., and Flamant, C.: Dynamical mechanisms controlling the vertical redistribution of dust and the thermodynamic structure of the West Saharan atmospheric boundary layer during summer, *Atmospheric Science Letters*, 10, 34–42, doi:10.1002/asl.207, 2009.
- 30 de Coëtlogon, G., Leduc-Leballeur, M., Meynadier, R., Bastin, S., Diakhaté, M., Eymard, L., Giordani, H., Janicot, S., and Lazar, A.: Atmospheric response to sea-surface temperature in the eastern equatorial Atlantic at quasi-biweekly time-scales, *Quarterly Journal of the Royal Meteorological Society*, 140, 1700–1714, doi:10.1002/qj.2250, 2014.
- 35 Dionisio, K. L., Rooney, M. S., Arku, R. E., Friedman, A. B., Hughes, A. F., Vallarino, J., Agyei-Mensah, S., Spengler, J. D., and Ezzati, M.: Within-Neighborhood Patterns and Sources of Particle Pollution: Mobile Monitoring and Geographic Information System Analysis in Four Communities in Accra, Ghana, *Environmental Health Perspectives*, 118, 607–613, doi:10.1289/ehp.0901365, 2010.

- Ek, M. B., Mitchell, K. E., Lin, Y., Rogers, E., Grunmann, P., Koren, V., Gayno, G., and Tarpley, J. D.: Implementation of Noah land surface model advances in the National Centers for Environmental Prediction operational mesoscale Eta model, *Journal of Geophysical Research: Atmospheres*, 108, n/a–n/a, doi:10.1029/2002JD003296, 2003.
- Flamant, C., Chaboureaud, J. P., Parker, D. J., Taylor, C. M., Cammas, J. P., Bock, O., Timouk, F., and Pelon, J.: Airborne observations of the impact of a convective system on the planetary boundary layer thermodynamics and aerosol distribution in the inter-tropical discontinuity region of the West African Monsoon, *Quarterly Journal of the Royal Meteorological Society*, 133, 1175–1189, doi:10.1002/qj.97, 2007.
- Flamant, C., Lavaysse, C., Todd, M. C., Chaboureaud, J. P., and Pelon, J.: Multi-platform observations of a springtime case of Bodele and Sudan dust emission, transport and scavenging over West Africa, *Quarterly Journal of the Royal Meteorological Society*, 135, 413–430, doi:10.1002/qj.376, 2009.
- Flaounas, E., Bastin, S., and Janicot, S.: Regional climate modelling of the 2006 West African monsoon: sensitivity to convection and planetary boundary layer parameterisation using WRF, *Climate Dynamics*, 36, 1083–1105, doi:10.1007/s00382-010-0785-3, 2010.
- Flaounas, E., Janicot, S., Bastin, S., and Roca, R.: The West African monsoon onset in 2006: sensitivity to surface albedo, orography, SST and synoptic scale dry-air intrusions using WRF, *Climate Dynamics*, 38, 685–708, doi:10.1007/s00382-011-1255-2, 2011.
- Folberth, G. a., Hauglustaine, D. a., Lathièrre, J., and Brocheton, F.: Interactive chemistry in the Laboratoire de Météorologie Dynamique general circulation model: model description and impact analysis of biogenic hydrocarbons on tropospheric chemistry, *Atmospheric Chemistry and Physics*, 6, 2273–2319, doi:10.5194/acp-6-2273-2006, 2006.
- Giglio, L., Csiszar, I., and Justice, C. O.: Global distribution and seasonality of active fires as observed with the Terra and Aqua Moderate Resolution Imaging Spectroradiometer (MODIS) sensors, *Journal of Geophysical Research: Biogeosciences*, 111, 1–12, doi:10.1029/2005JG000142, 2006.
- Guenther, a., Karl, T., Harley, P., Wiedinmyer, C., Palmer, P. I., and Geron, C.: Estimates of global terrestrial isoprene emissions using MEGAN (Model of Emissions of Gases and Aerosols from Nature), *Atmospheric Chemistry and Physics Discussions*, 6, 107–173, doi:10.5194/acpd-6-107-2006, 2006.
- Hadji, E., Doumbia, T., Liousse, C., Galy-lacaux, C., Ababacar, S., Diop, B., Ouafu, M., Michel, E., Gardrat, E., Castera, P., Rosset, R., Akpo, A., and Sighe, L.: Real time black carbon measurements in West and Central Africa urban sites, *Atmospheric Environment*, 54, 529–537, doi:10.1016/j.atmosenv.2012.02.005, 2012.
- Hall, N. and Peyrillé, P.: Dynamics of the West African monsoon, *Journal de Physique IV*, 139, 81–99, doi:10.1051/jp4, 2006.
- Haywood, J. M., Pelon, J., Formenti, P., Bharmal, N., Brooks, M., Capes, G., Chazette, P., Chou, C., Christopher, S., Coe, H., Cuesta, J., Derimian, Y., Desboeufs, K., Greed, G., Harrison, M., Heese, B., Highwood, E. J., Johnson, B., Mallet, M., Marticorena, B., Marsham, J., Milton, S., Myhre, G., Osborne, S. R., Parker, D. J., Rajot, J. L., Schulz, M., Slingo, A., Tanre, D., and Tulet, P.: Overview of the Dust and Biomass-burning Experiment and African Monsoon Multidisciplinary Analysis Special Observing Period-0, *Journal of Geophysical Research-Atmospheres*, 113, 20, doi:10.1029/2008jd010077, 2008.
- Holben, B. N., Eck, T. F., Slutsker, I., Tanre, D., Buis, J. P., Setzer, A., Vermote, E., Reagan, J. A., Kaufman, Y. J., Nakajima, T., Lavenue, F., Jankowiak, I., and Smirnov, A.: AERONET - A federated instrument network and data archive for aerosol characterization, *Remote Sensing of Environment*, 66, 1–16, doi:10.1016/s0034-4257(98)00031-5, 1998.
- Hong, S. and Lim, J.: The WRF single-moment 6-class microphysics scheme (WSM6), 2006.
- Hong, S.-Y., Noh, Y., and Dudhia, J.: A new vertical diffusion package with an explicit treatment of entrainment processes., *Monthly Weather Review*, 134, 2318–2341, doi:10.1175/MWR3199.1, 2006.

- Janicot, S., Thorncroft, C. D., Ali, A., Asencio, N., Berry, G., Bock, O., Bourles, B., Caniaux, G., Chauvin, F., Deme, A., Kergoat, L., Lafore, J.-P., Lavaysse, C., Lebel, T., Marticorena, B., Mounier, F., Nedelec, P., Redelsperger, J.-L., Ravegnani, F., Reeves, C. E., Roca, R., de Rosnay, P., Schlager, H., Sultan, B., Tomasini, M., and Ulanovsky, A.: Large-scale overview of the summer monsoon over West Africa during the AMMA field experiment in 2006, doi:10.5194/angeo-26-2569-2008, 2008.
- 5 Karam, D. B., Flamant, C., Tulet, P., Chaboureaud, J. P., Dabas, A., and Todd, M. C.: Estimate of Sahelian dust emissions in the intertropical discontinuity region of the West African Monsoon, *Journal of Geophysical Research: Atmospheres*, 114, D13 106, doi:10.1029/2008JD011444, 2009.
- Knippertz, P., Coe, H., Chiu, J. C., Evans, M. J., Fink, A. H., Kalthoff, N., Lioussé, C., Mari, C., Allan, R. P., Brooks, B., Danour, S., Flamant, C., Jegede, O. O., Lohou, F., and Marsham, J. H.: The DACCWA project: Dynamics-aerosol-chemistry-cloud interactions in West Africa, *Bulletin of the American Meteorological Society*, p. 150203142711003, doi:10.1175/BAMS-D-14-00108.1, 2015.
- 10 Lafore, J.-P., Flamant, C., Guichard, F., Parker, D. J., Bouniol, D., Fink, a. H., Giraud, V., Gosset, M., Hall, N., Höller, H., Jones, S. C., Protat, a., Roca, R., Roux, F., Saïd, F., and Thorncroft, C.: Progress in understanding of weather systems in West Africa, *Atmospheric Science Letters*, 12, 7–12, doi:10.1002/asl.335, 2011.
- Lavaysse, C., Flamant, C., Janicot, S., Parker, D., Lafore, J. P., Sultan, B., and Pelon, J.: Seasonal evolution of the West African heat low: a climatological perspective, *Climate Dynamics*, 33, 313–330, 2009.
- 15 Leduc-Leballeur, M., de Coëtlogon, G., and Eymard, L.: Air-sea interaction in the Gulf of Guinea at intraseasonal time-scales: Wind bursts and coastal precipitation in boreal spring, *Quarterly Journal of the Royal Meteorological Society*, 139, 387–400, doi:10.1002/qj.1981, 2013.
- Lelieveld, J., Evans, J. S., Fnais, M., Giannadaki, D., and Pozzer, A.: The contribution of outdoor air pollution sources to premature mortality on a global scale., *Nature*, 525, 367–71, doi:10.1038/nature15371, 2015.
- 20 Li, R., Jin, J., Wang, S.-Y., and Gillies, R. R.: Significant impacts of radiation physics in the Weather Research and Forecasting model on the precipitation and dynamics of the West African Monsoon, *Climate Dynamics*, 44, 1583–1594, doi:10.1007/s00382-014-2294-2, 2015.
- Lindén, J., Thorsson, S., and Eliasson, I.: Carbon monoxide in Ouagadougou, Burkina Faso - A comparison between urban background, roadside and in-traffic measurements, *Water, Air, and Soil Pollution*, 188, 345–353, doi:10.1007/s11270-007-9538-2, 2008.
- 25 Lindén, J., Boman, J., Holmer, B., Thorsson, S., and Eliasson, I.: Intra-urban air pollution in a rapidly growing Sahelian city, *Environment International*, 40, 51–62, doi:10.1016/j.envint.2011.11.005, 2012.
- Lioussé, C., Guillaume, B., Grégoire, J. M., Mallet, M., Galy, C., Pont, V., Akpo, a., Bedou, M., Castéra, P., Dungall, L., Gardrat, E., Granier, C., Konaré, a., Malavelle, F., Mariscal, a., Mieville, a., Rosset, R., Serça, D., Solmon, F., Tummon, F., Assamoi, E., Yoboué, V., and Van Velthoven, P.: Updated African biomass burning emission inventories in the framework of the AMMA-IDAF program, with an evaluation of combustion aerosols, *Atmospheric Chemistry and Physics*, 10, 9631–9646, doi:10.5194/acp-10-9631-2010, 2010.
- 30 Lioussé, C., Assamoi, E., Criqui, P., Granier, C., and Rosset, R.: Explosive growth in African combustion emissions from 2005 to 2030, *Environmental Research Letters*, 9, 035 003, doi:10.1088/1748-9326/9/3/035003, 2014.
- Lothon, M., Saïd, F., Lohou, F., and Campistron, B.: Observation of the Diurnal Cycle in the Low Troposphere of West Africa, *Monthly Weather Review*, 136, 3477–3500, doi:10.1175/2008MWR2427.1, 2008.
- 35 Mailler, S., Menut, L., Khvorostyanov, D., Valari, M., Couvidat, F., Siour, G., Turquety, S., Briant, R., Tuccella, P., Bessagnet, B., Collette, A., Létinois, L., and Meleux, F.: CHIMERE-2016: From urban to hemispheric chemistry-transport modeling, *Geoscientific Model Development Discussions*, 0, 1–41, doi:10.5194/gmd-2016-196, 2016.

- Marais, E., Jacob, D., Wecht, K., Lerot, C., Zhang, L., Yu, K., Kurosu, T., Chance, K., and Sauvage, B.: Anthropogenic emissions in Nigeria and implications for atmospheric ozone pollution: A view from space, *Atmospheric Environment*, 99, 32–40, doi:10.1016/j.atmosenv.2014.09.055, 2014.
- Mari, C. H., Cailley, G., Corre, L., Saunois, M., Attié, J. L., Thouret, V., and Stohl, a.: Tracing biomass burning plumes from the Southern Hemisphere during the AMMA 2006 wet season experiment, *Atmospheric Chemistry and Physics Discussions*, 7, 17 339–17 366, doi:10.5194/acpd-7-17339-2007, 2007.
- Mari, C. H., Reeves, C. E., Law, K. S., Ancellet, G., Andrés-Hernández, M. D., Barret, B., Bechara, J., Borbon, A., Bouarar, I., Cairo, F., Commane, R., Delon, C., Evans, M. J., Fierli, F., Floquet, C., Galy-Lacaux, C., Heard, D. E., Homan, C. D., Ingham, T., Larsen, N., Lewis, A. C., Liousse, C., Murphy, J. G., Orlandi, E., Oram, D. E., Saunois, M., Serça, D., Stewart, D. J., Stone, D., Thouret, V., Velthoven, P. V., and Williams, J. E.: Atmospheric composition of West Africa: Highlights from the AMMA international program, *Atmospheric Science Letters*, 12, 13–18, doi:10.1002/asl.289, 2011.
- Marticorena, B., Chatenet, B., Rajot, J. L., Traore, S., Coulibaly, M., Diallo, A., Kone, I., Maman, A., Diaye, T. N., and Zakou, A.: Temporal variability of mineral dust concentrations over West Africa: analyses of a pluriannual monitoring from the AMMA Sahelian Dust Transect, *Atmospheric Chemistry and Physics*, 10, 8899–8915, doi:10.5194/acp-10-8899-2010, 2010.
- Menut, L., Chiapello, I., and Moulin, C.: Predictability of mineral dust concentrations: The African Monsoon Multidisciplinary Analysis first short observation period forecasted with CHIMERE-DUST, *Journal of Geophysical Research: Atmospheres*, 114, 1–13, doi:10.1029/2008JD010523, 2009.
- Menut, L., Bessagnet, B., Khvorostyanov, D., Beekmann, M., Blond, N., Colette, a., Coll, I., Curci, G., Foret, G., Hodzic, a., Mailler, S., Meleux, F., Monge, J.-L., Pison, I., Siour, G., Turquety, S., Valari, M., Vautard, R., and Vivanco, M. G.: CHIMERE 2013: a model for regional atmospheric composition modelling, *Geoscientific Model Development*, 6, 981–1028, doi:10.5194/gmd-6-981-2013, 2013a.
- Menut, L., Pérez, C., Haustein, K., Bessagnet, B., Prigent, C., and Alfaro, S.: Impact of surface roughness and soil texture on mineral dust emission fluxes modeling, *Journal of Geophysical Research: Atmospheres*, 118, 6505–6520, doi:10.1002/jgrd.50313, 2013b.
- Menut, L., Siour, G., Mailler, S., Couvidat, F., and Bessagnet, B.: Observations and regional modeling of aerosol optical properties, speciation and size distribution over Northern Africa and western Europe, *Atmospheric Chemistry and Physics*, 16, 12 961–12 982, doi:10.5194/acp-16-12961-2016, 2016.
- Meynadier, R., de Coëtlogon, G., Leduc-Leballeur, M., Eymard, L., and Janicot, S.: Seasonal influence of the sea surface temperature on the low atmospheric circulation and precipitation in the eastern equatorial Atlantic, *Climate Dynamics*, 47, 1127–1142, doi:10.1007/s00382-015-2892-7, 2016.
- Minga, a., Thouret, V., Saunois, M., Delon, C., Serça, D., Mari, C., Sauvage, B., Mariscal, a., Leriche, M., and Cros, B.: What caused extreme ozone concentrations over Cotonou in December 2005?, *Atmospheric Chemistry and Physics Discussions*, 9, 21 011–21 039, doi:10.5194/acpd-9-21011-2009, 2009.
- Mlawer, E. J., Taubman, S. J., Brown, P. D., Iacono, M. J., and Clough, S. a.: Radiative transfer for inhomogeneous atmospheres: RRTM, a validated correlated-k model for the longwave, *Journal of Geophysical Research*, 102, 16 663, doi:10.1029/97JD00237, 1997.
- Ndoke, P. and Jimoh, O.: Impact of traffic emission on air quality in a developing city of Nigeria, *Assumpt Univ J Technol*, pp. 222–227, 2005.
- Ogunjobi, K. O., He, Z., and Simmer, C.: Spectral aerosol optical properties from AERONET Sun-photometric measurements over West Africa, *Atmospheric Research*, 88, 89–107, doi:10.1016/j.atmosres.2007.10.004, 2008.

- Parker, D. J., Burton, R. R., Diongue-Niang, A., Ellis, R. J., Felton, M., Taylor, C. M., Thorncroft, C. D., Bessemoulin, P., and Tompkins, a. M.: The diurnal cycle of the West African monsoon circulation, *Quarterly Journal of the Royal Meteorological Society*, 131, 2839–2860, doi:10.1256/qj.04.52, 2005.
- Péré, J., Mallet, M., Pont, V., and Bessagnet, B.: *Atmospheric Environment*, 44, 3688–3699, doi:10.1016/j.atmosenv.2010.06.034, 2010.
- 5 Péré, J. C., Mallet, M., Bessagnet, B., and Pont, V.: Evidence of the aerosol core-shell mixing state over Europe during the heat wave of summer 2003 by using CHIMERE simulations and AERONET inversions, *Geophysical Research Letters*, 36, L09 807, doi:10.1029/2009GL037334, 2009.
- Pospichal, B., Karam, D., Crewell, S., Flamant, C., Hünerbein, A., Bock, O., and Saïd, F.: Diurnal cycle of the intertropical discontinuity over West Africa analysed by remote sensing and mesoscale modelling, *Quarterly Journal of the Royal Meteorological Society*, 136, 92–106, doi:10.1002/qj.435, 2010.
- 10 Redelsperger, J. L., Thorncroft, C. D., Diedhiou, A., Lebel, T., Parker, D. J., and Polcher, J.: The African Monsoon Multidisciplinary Analysis: An International Research Project and Field Campaign, *Bulletin of the American Meteorological Society*, 87, 1739–1746, 2006.
- Reeves, C. E., Formenti, P., Afif, C., Ancellet, G., Attié, J. L., Bechara, J., Borbon, A., Cairo, F., Coe, H., Crumeyrolle, S., Fierli, F., Flamant, C., Gomes, L., Hamburger, T., Jambert, C., Law, K. S., Mari, C., Jones, R. L., Matsuki, A., Mead, M. I., Methven, J., Mills, G. P., Minikin, A., Murphy, J. G., Nielsen, J. K., Oram, D. E., Parker, D. J., Richter, A., Schlager, H., Schwarzenboeck, A., and Thouret, V.: Chemical and aerosol characterisation of the troposphere over West Africa during the monsoon period as part of AMMA, *Atmospheric Chemistry and Physics*, 10, 7575–7601, doi:10.5194/acp-10-7575-2010, 2010.
- 15 Sauvage, B., Thouret, V., Cammas, J.-P., Gheusi, F., Athier, G., and Nédélec, P.: Tropospheric ozone over Equatorial Africa: regional aspects from the MOZAIC data, *Atmospheric Chemistry and Physics Discussions*, 4, 3285–3332, doi:10.5194/acpd-4-3285-2004, 2004.
- 20 Schmechtig, C., Marticorena, B., Chatenet, B., Bergametti, G., Rajot, J. L., and Coman, A.: Simulation of the mineral dust content over Western Africa from the event to the annual scale with the CHIMERE-DUST model, *Atmos. Chem. Phys.*, 11, 7185–7207, 2011.
- Schwendike, J., Kalthoff, N., and Kohler, M.: The impact of mesoscale convective systems on the surface and boundary-layer structure in West Africa: Case-studies from the AMMA campaign 2006, *Quarterly Journal of the Royal Meteorological Society*, pp. n/a–n/a, doi:10.1002/qj.599, 2010.
- 25 Skamarock, W. C. and Klemp, J. B.: A time-split nonhydrostatic atmospheric model for weather research and forecasting applications, *Journal of Computational Physics*, 227, 3465–3485, doi:10.1016/j.jcp.2007.01.037, 2008.
- Sultan, B. and Janicot, S.: Abrupt shift of the ITCZ over West Africa and intra-seasonal variability, *Geophysical Research Letters*, 27, 3353–3356, 2000.
- Sultan, B. and Janicot, S.: The West African monsoon dynamics. Part II: The 'preonset' and 'onset' of the summer monsoon, *Journal of Climate*, 16, 3407–3427, 2003.
- 30 Sultan, B., Janicot, S., and Diedhiou, A.: The West African Monsoon Dynamics. Part I: Documentation of Intraseasonal Variability, *Journal of Climate*, 16, 3389–3406, doi:10.1175/1520-0442(2003)0162.0.CO, 2003.
- Turquety, S., Menut, L., Bessagnet, B., Anav, a., Viovy, N., Maignan, F., and Wooster, M.: APIFLAME v1.0: high resolution fire emission model and application to the Euro-Mediterranean region, *Geoscientific Model Development Discussions*, 6, 5489–5551, doi:10.5194/gmdd-6-5489-2013, 2013.
- 35 von Storch, H., Langenberg, H., and Feser, F.: A Spectral Nudging Technique for Dynamical Downscaling Purposes, *Monthly Weather Review*, 128, 3664–3673, doi:10.1175/1520-0493(2000)128<3664:ASNTFD>2.0.CO;2, 2000.

Williams, J. E., Scheele, M. P., Van Velthoven, P. F. J., Thouret, V., Saunois, M., and Reeves, C. E.: The influence of biomass burning and transport on tropospheric composition over the tropical Atlantic Ocean and Equatorial Africa during the West African monsoon in 2006, *Atmospheric Chemistry and Physics*, 10, 9797–9817, doi:10.5194/acp-10-9797-2010, 2010.

Zhu, X. R.: GAW Report No. 205 WMO-IGAC Impacts of Megacities on Air Pollution and Climate, Tech. Rep. 205, 2012.

List of Figures

- 1 Anthropogenic carbon monoxide (top) and primary particulate matter (bottom) surface emission fluxes in $\text{kg.km}^{-2}.\text{day}^{-1}$ averaged over the three months period. The gray dots are the major cities and the three green dots are the locations studied from the South to the North: Cotonou (Benin), Djougou (Benin), Niamey (Niger). The blue box represents the Cotonou (Benin) - Niamey (Niger) meridional transect studied (longitude $\lambda = 2^\circ$ East to 3° East, latitude $\phi = 1^\circ$ North to 19° North). 28
- 2 Time-latitude average (Hovmöller) of precipitation (mm.day^{-1}). Precipitation is averaged between 8.5°W and 8.5°E in longitude. Day-to-day variability is eliminated by applying a moving average of ± 2 days. Due to the longitudinal average, the coastline is between 5°N and 6°N . The 2 gray lines show the latitudinal extend of the regional model domain. The 3 dash gray lines present the latitudes of the 3 locations studied (Cotonou, Djougou and Niamey). 29
- 3 Observed daily averages of AERONET level 2 AOD and Angström exponent (black dots) at Djougou (Benin) and Banizoumbou compared to the modeled time series with a splitting to extract the relative contribution between without biomass burning emissions (including anthropogenic, biogenic, sea salt and mineral dust); all ~~three~~ four in blue) and with biomass burning emissions (in red). 30
- 4 (top) EUMETSAT visible image of the Cotonou area of the 13 June 2006 at 20 UTC (from NAScube (<http://nascube.univ-lille1.fr>); (bottom) Map of Cotonou area for the 13 June 2006 at 12 UTC with wind vectors at 10 m (orange arrows), precipitation (blue shading). The two flight trajectories are displayed with the red line for the 13 June and with the green line for the 14 June. 31
- 5 Time-latitude average (Hovmöller diagram) of: a) surface CO concentration (ppb), and b) $\text{PM}_{2.5}$ ($\mu\text{g.m}^{-3}$) due to anthropogenic emissions along a meridional transect from 2°N to 19°N and averaged from 2°E to 3°E including Cotonou (Benin) and Niamey (Niger). Day-to-day variability is smoothed by applying a moving average of ± 2 days. White contours are precipitation = 10 mm.day^{-1} . Specific isocontours are highlighted = $4 \mu\text{g.m}^{-3}$ (orange) and $= 5 \mu\text{g.m}^{-3}$ (~~pink~~violet). The black line is the ITD defined as RH isocontour = 20 %. 32
- 6 Time-latitude average (Hovmöller diagram) of surface wind: a) speed and b) direction, along a meridional transect from 2°N to 19°N and averaged from 2°E to 3°E including Cotonou (Benin) and Niamey (Niger). Wind directions are presented with steps of 45° . Day-to-day variability is smoothed by applying a moving average of ± 2 days. Orange and ~~pink~~violet contours are surface $\text{PM}_{2.5}$ concentrations of 4 and $5 \mu\text{g.m}^{-3}$ 33
- 7 Vertical cross-section of the meridional wind (shading in m.s^{-1}) mean over: a) May, b) June and c) July, at 00 UTC along a meridional transect from 2°N to 19°N and averaged from 2°E to 3°E including Cotonou (Benin) and Niamey (Niger). ~~Light orange, orange~~ Orange and ~~pink~~violet shading ~~represents~~ represent anthropogenic $\text{PM}_{2.5}$ ~~concentration concentrations of~~ $= 3.0 \mu\text{g.m}^{-3}$, $= 4.0 \mu\text{g.m}^{-3}$ and $= 5.0 \mu\text{g.m}^{-3}$. Vectors ~~are vertical and meridional~~ represent the wind field in the plan of the transect (with an aspect ratio of 500 between the meridional and the vertical components). The green line is the PBL height (m). The grey vertical dash line is the latitude of the coast. 34
- 8 Vertical cross-section of the meridional wind (shading in m.s^{-1}) along a meridional transect from 2°N to 19°N ~~and~~ averaged from 2°E to 3°E including Cotonou (Benin) and Niamey (Niger) ; and averaged over 20 to 30 June at 00 UTC. Isocontours represent gaseous tracers concentration continuously emitted (in arbitrary unit) from the 1 to 30 June at: a) Niamey (Niger) and b) Cotonou (Benin). Brown ~~yellow~~ yellow and ~~white~~ white shading represent tracers concentration = 1 a.u. ~~and~~ $= 10\%$ a.u. and $= 1\%$ respectively. ~~u.~~ The green line is the PBL height (m). Vectors represent the wind field in the plan of the transect (with an aspect ratio of 500 between the meridional and the vertical components). The white vertical dash line is the latitude of the coast. 35
- 9 Time-latitude average (Hovmöller) of surface anthropogenic $\text{PM}_{2.5}$ concentration ($\mu\text{g.m}^{-3}$) averaged along a meridional transect between 2°East and 3°East from 1 to 17 June 2016. Black vertical bars delimit the periods of the day (00 UTC; 06 UTC; 12 UTC; 18 UTC). White isocontours present precipitation rate = 3.0 mm.hour^{-1}). Orange isocontour represents the surface anthropogenic $\text{PM}_{2.5}$ concentration = $4 \mu\text{g.m}^{-3}$ 36

10	Time-latitude average (Hovmöller) of gaseous tracers concentration (a.u.) averaged along a meridional transect between 2°E and 3°E centered on Cotonou (Benin) from 8 to 15 June 2006. Emissions are set up with a constant emission between 0 m and 500 m altitude at: a) Cotonou (Benin), b) Lome (Togo) and c) Accra (Ghana). Black vertical bars delimit the periods of the day (00 UTC; 06 UTC; 12 UTC; 18 UTC).	37
5	11 Vertical cross-section of the meridional wind (shading in m.s^{-1}) along a meridional transect from 5°N to 10°N and averaged from 2°E to 3°E including Cotonou (Benin). The two orange isocontours are tracer concentrations released in Cotonou and in Lome, respectively bold and dashed, with same threshold values (in arbitrary unit). Vectors are vertical and meridional <u>represent the wind field in the plan of the transect</u> (with an aspect ratio of 500 <u>between the meridional and the vertical components</u>). The green line is the PBL height (m). The white vertical dash line is the latitude of the coast.	38
10	12 EUMETSAT visible image of the Cotonou area of the 11 June 2006 at 19 UTC (from NAScube (http://nascube.univ-lille1.fr). <u>The red ellipse is the convective cell location.</u>	39
15	13 (top) Map of Cotonou area for the 11 June 2006 at 19UTC <u>19 UTC</u> with wind vectors at 10 m (green arrows), precipitation (blue shading), anthropogenic $\text{PM}_{2.5}$ concentration (red shading); (bottom) Isocontours of tracers concentration on 11 June at 19 UTC (solid line) and on 12 June at 01 UTC (dashed line), released in Accra (Ghana) in green, Lome (Togo) in red, Cotonou (Benin) in orange, Lagos (Nigeria) in violet. Blue dots show precipitation location each hour between 11 June at 19 UTC and on 12 June at 01 UTC (the size of blue dots depends on precipitation amount).	40

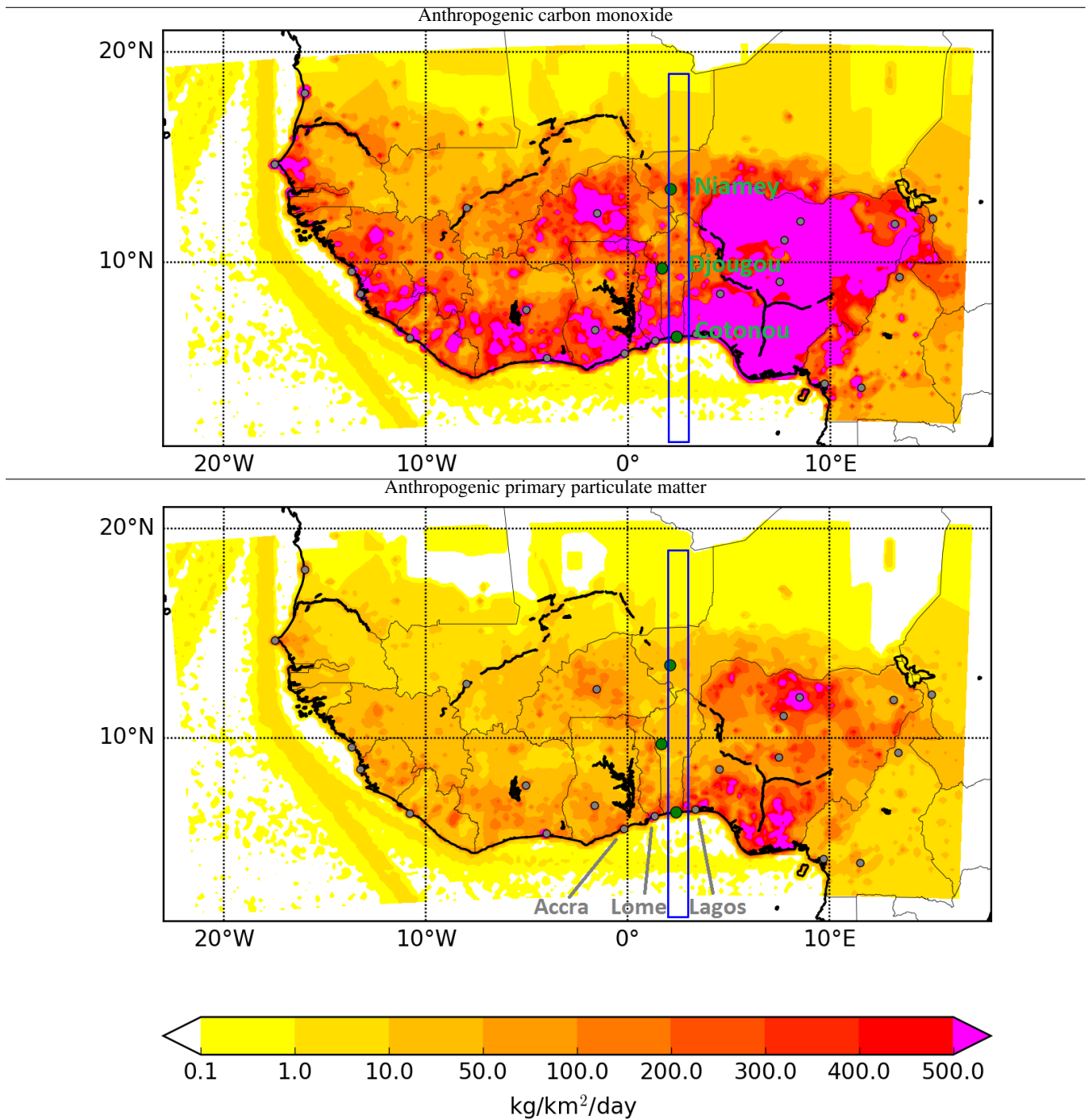


Figure 1. Anthropogenic carbon monoxide (top) and primary particulate matter (bottom) surface emission fluxes in $\text{kg.km}^{-2}.\text{day}^{-1}$ averaged over the three months period. The gray dots are the major cities and the three green dots are the locations studied from the South to the North: Cotonou (Benin), Djougou (Benin), Niamey (Niger). The blue box represents the Cotonou (Benin) - Niamey (Niger) meridional transect studied (longitude $\lambda = 2^\circ$ East to 3° East, latitude $\phi = 1^\circ$ North to 19° North).

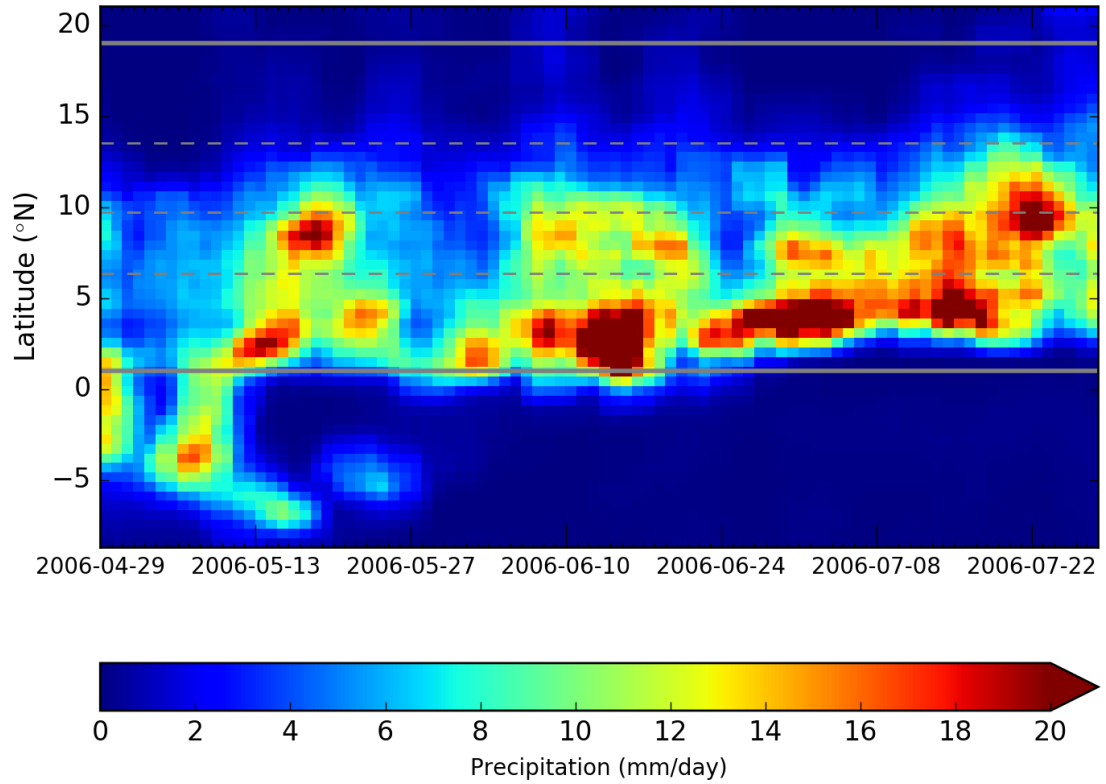


Figure 2. Time-latitude average (Hovmöller) of precipitation (mm.day^{-1}). Precipitation is averaged between 8.5°W and 8.5°E in longitude. Day-to-day variability is eliminated by applying a moving average of ± 2 days. Due to the longitudinal average, the coastline is between 5°N and 6°N . The 2 gray lines show the latitudinal extend of the regional *model* domain. The 3 dash gray lines present the latitudes of the 3 locations studied (Cotonou, Djougou and Niamey).

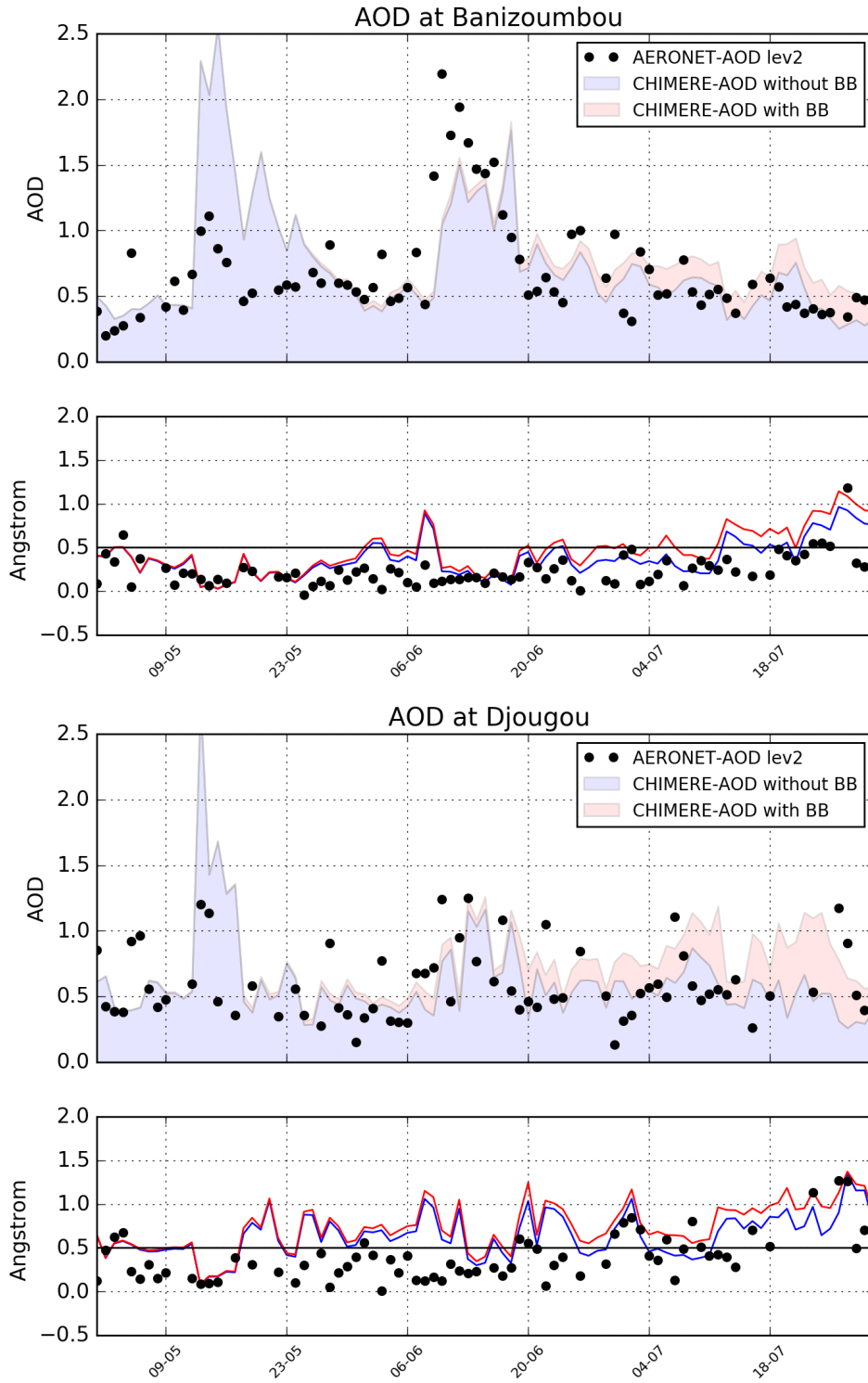


Figure 3. Observed daily averages of AERONET level 2 AOD and Angström exponent (black dots) at Djougou (Benin) and Banizoumbou compared to the modeled time series with a splitting to extract the relative contribution between without biomass burning emissions (including anthropogenic, biogenic, sea salt and mineral dust) (in blue) and with biomass burning emissions (in red).

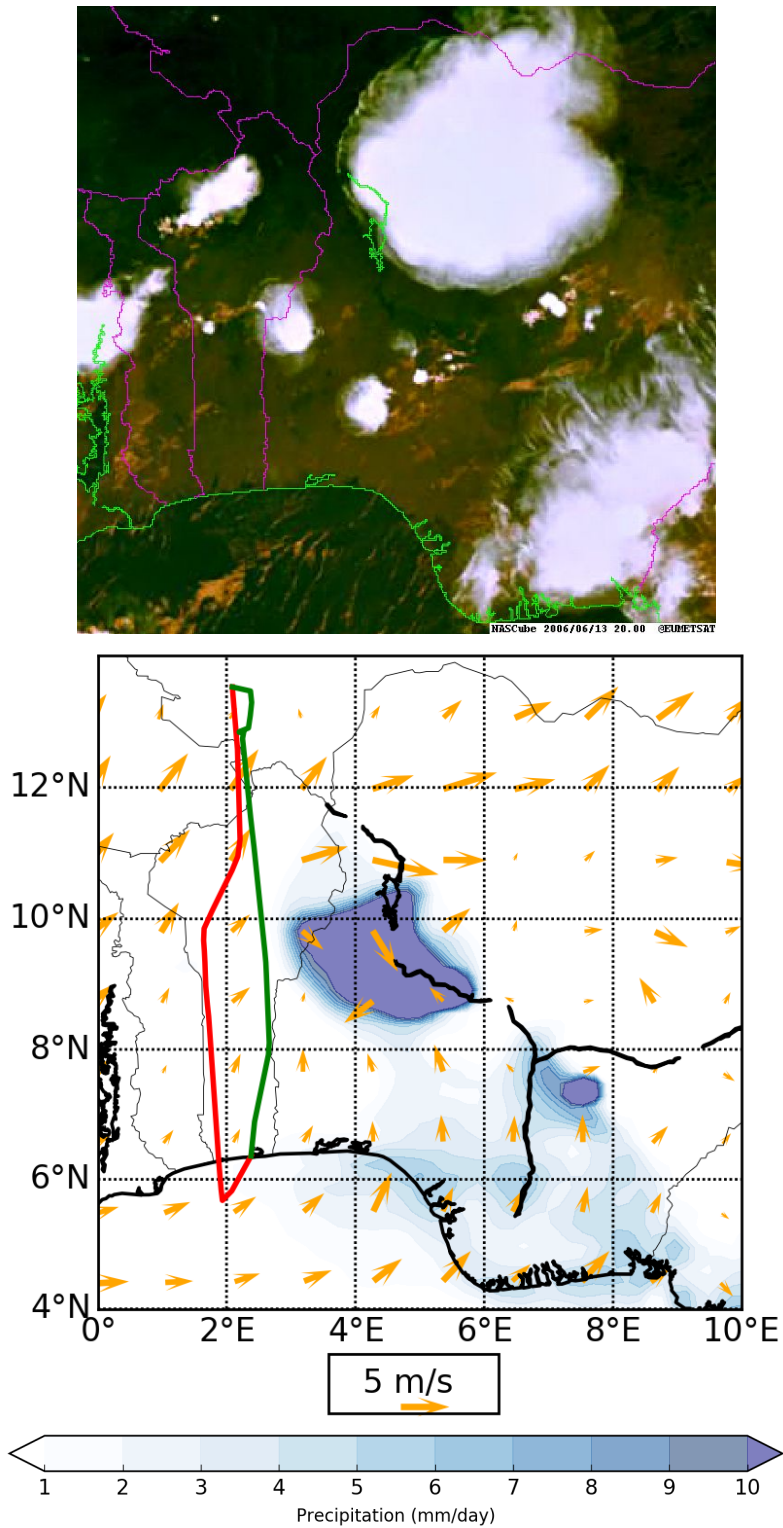


Figure 4. (top) EUMETSAT visible image of the Cotonou area of the 13 June 2006 at 20 UTC (from NAScube (<http://nascube.univ-lille1.fr>); (bottom) Map of Cotonou area for the 13 June 2006 at 12 UTC with wind vectors at 10 m (orange arrows), precipitation (blue shading). The two flight trajectories are displayed with the red line for the 13 June and with the green line for the 14 June.

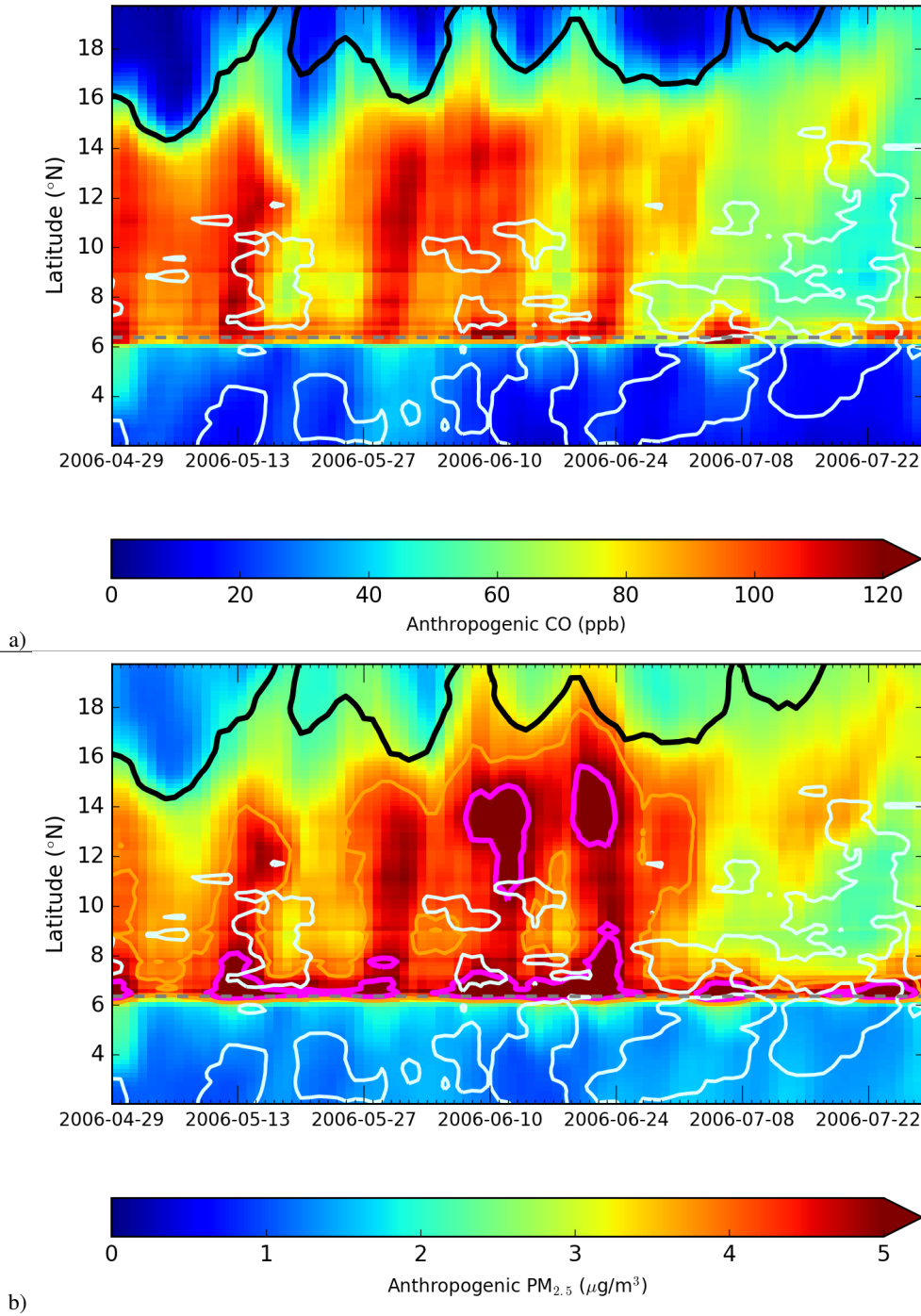
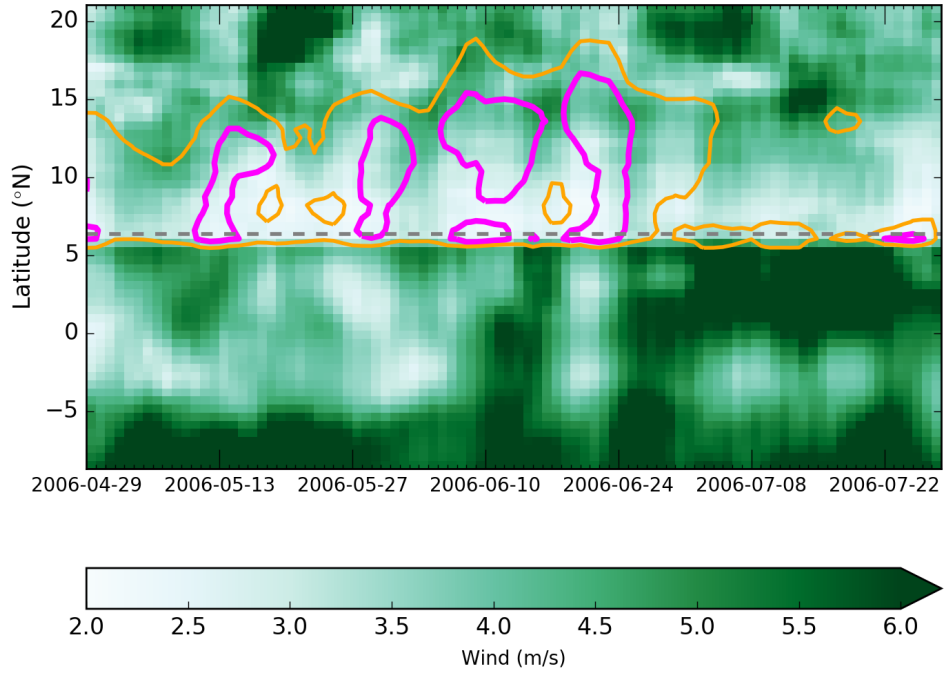
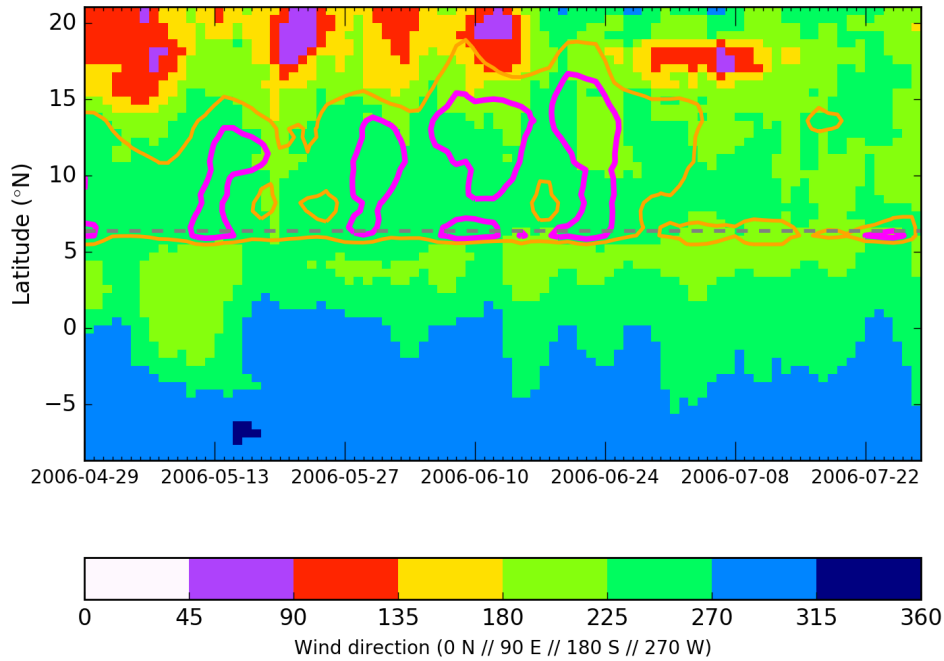


Figure 5. Time-latitude average (Hovmöller diagram) of: a) surface CO concentration (ppb), and b) $PM_{2.5}$ ($\mu\text{g.m}^{-3}$) due to anthropogenic emissions along a meridional transect from 2°N to 19°N and averaged from 2°E to 3°E including Cotonou (Benin) and Niamey (Niger). Day-to-day variability is smoothed by applying a moving average of ± 2 days. White contours are precipitation = 10 mm.day^{-1} . Specific isocontours are highlighted = $4 \mu\text{g.m}^{-3}$ (orange) and = $5 \mu\text{g.m}^{-3}$ (pink/violet). The black line is the ITD defined as RH isocontour = 20 %.



a)



b)

Figure 6. Time-latitude average (Hovmöller diagram) of surface wind: a) speed and b) direction, along a meridional transect from 2°N to 19°N and averaged from 2°E to 3°E including Cotonou (Benin) and Niamey (Niger). Wind directions are presented with steps of 45°. Day-to-day variability is smoothed by applying a moving average of ± 2 days. Orange and pink-violet contours are surface PM_{2.5} concentrations of 4 and 5 $\mu\text{g.m}^{-3}$.

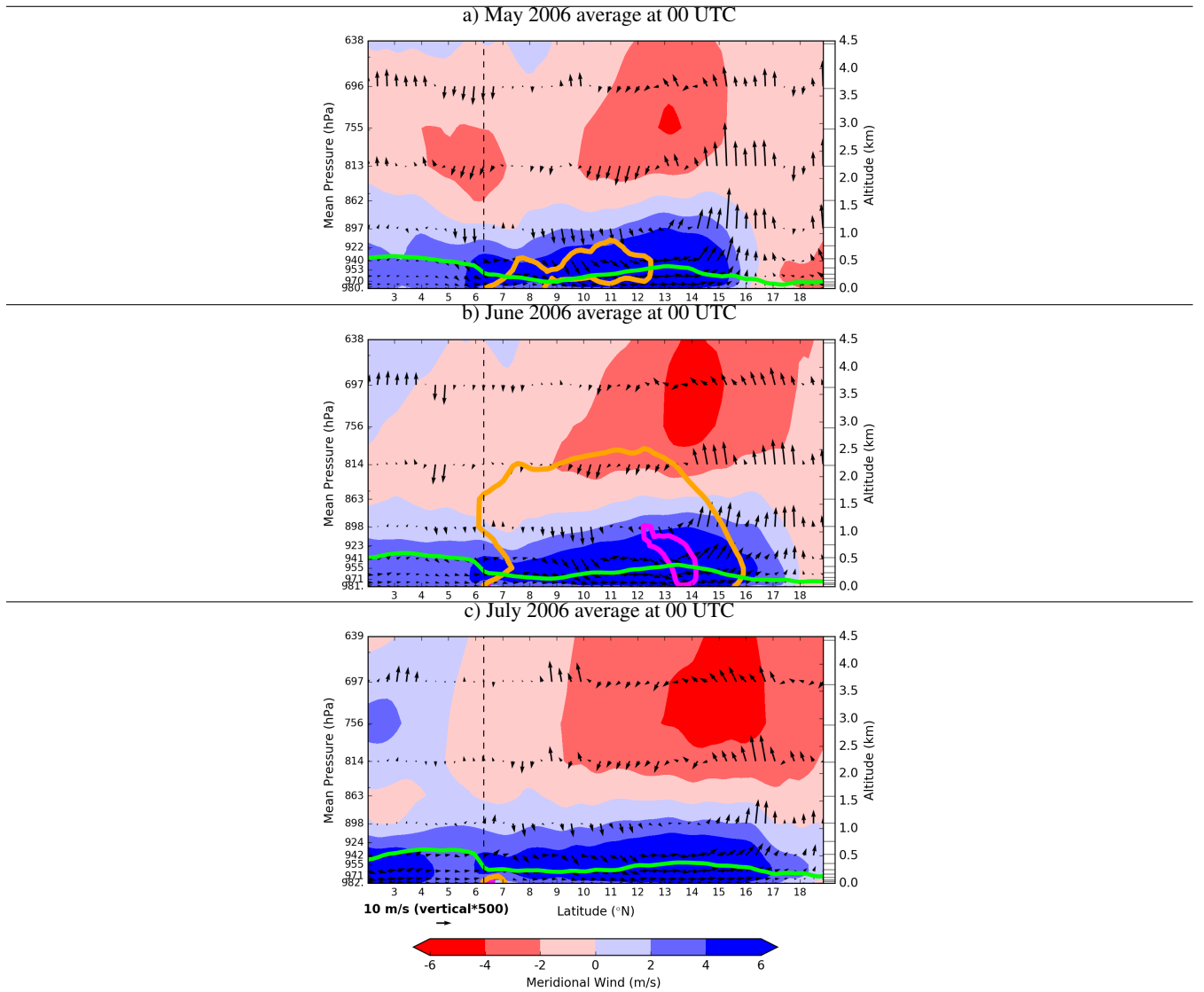
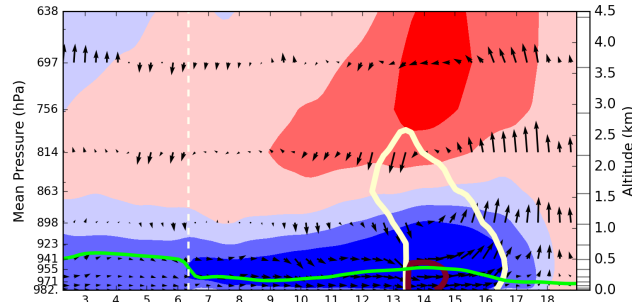


Figure 7. Vertical cross-section of the meridional wind (shading in $m.s^{-1}$) mean over: a) May, b) June and c) July, at 00 UTC along a meridional transect from 2 $^{\circ}N$ to 19 $^{\circ}N$ and averaged from 2 $^{\circ}E$ to 3 $^{\circ}E$ including Cotonou (Benin) and Niamey (Niger). Light orange, orange and pink-violet shading represents anthropogenic $PM_{2.5}$ concentration concentrations of = 3.0 $\mu g.m^{-3}$, = 4.0 $\mu g.m^{-3}$ and = 5.0 $\mu g.m^{-3}$. Vectors are vertical and meridional represent the wind field in the plan of the transect (with an aspect ratio of 500 between the meridional and the vertical components). The green line is the PBL height (m). The grey vertical dash line is the latitude of the coast.

a) Niamey (Niger) tracers emission averaged at 00 UTC



b) Cotonou (Benin) tracers emission averaged at 00 UTC

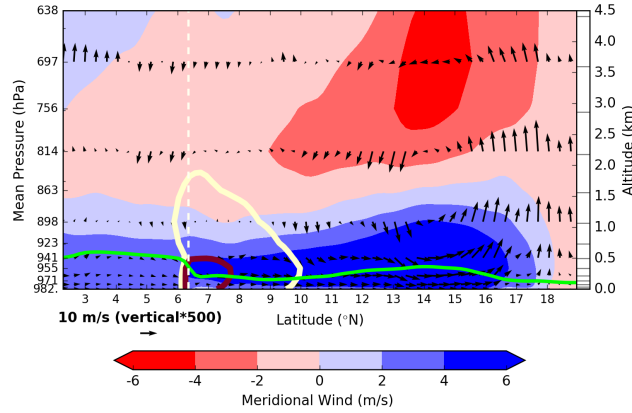


Figure 8. Vertical cross-section of the meridional wind (shading in m.s^{-1}) along a meridional transect from 2°N to 19°N and, averaged from 2°E to 3°E including Cotonou (Benin) and Niamey (Niger), averaged over 20 to 30 June at 00 UTC. Isocontours represent gaseous tracers concentration continuously emitted (in arbitrary unit) from the 1 to 30 June at: a) Niamey (Niger) and b) Cotonou (Benin). Brown, yellow and white-yellow shading represent tracers concentration = 1 a.u., 10 % a.u. and 1 % a.u. respectively. The green line is the PBL height (m). Vectors represent the wind field in the plan of the transect (with an aspect ratio of 500 between the meridional and the vertical components). The white vertical dash line is the latitude of the coast.

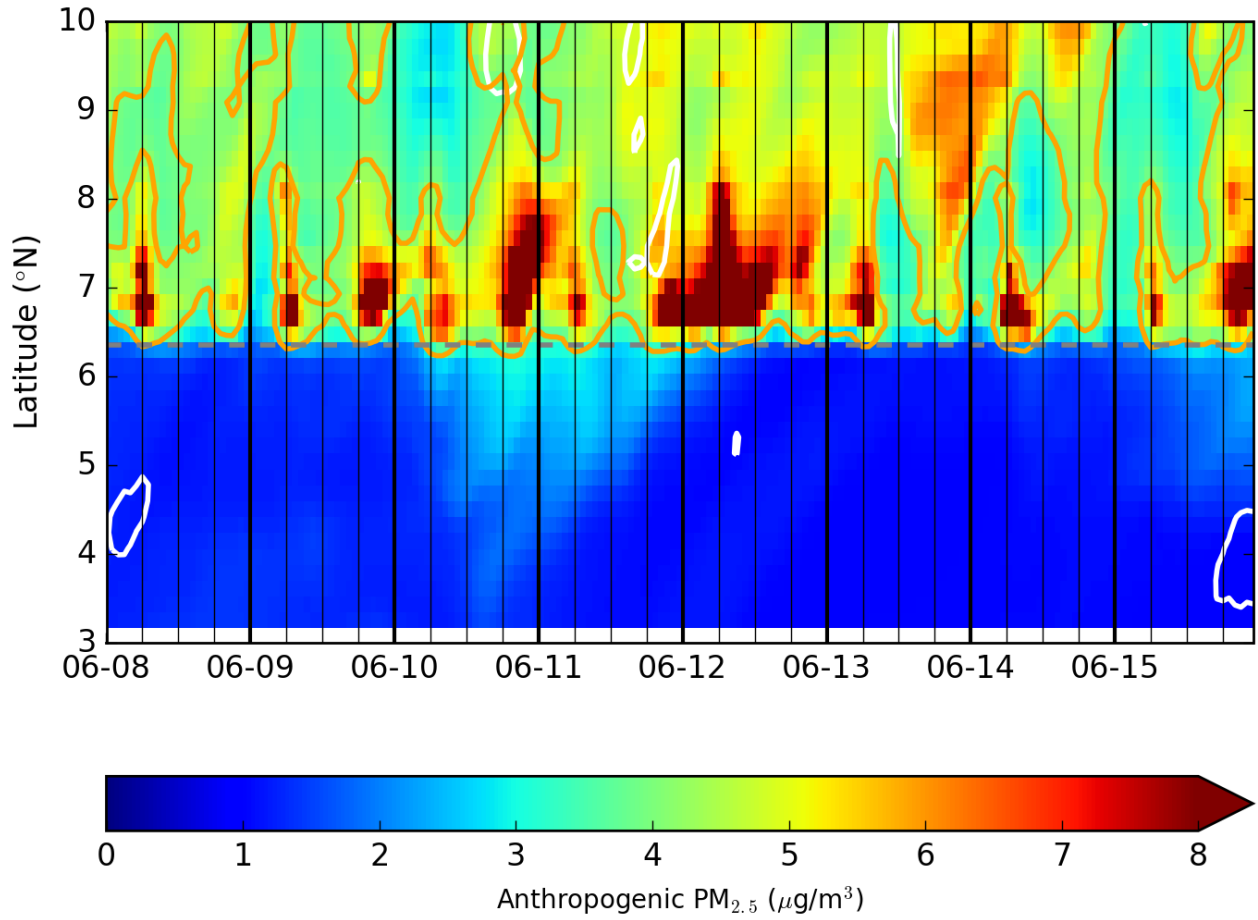
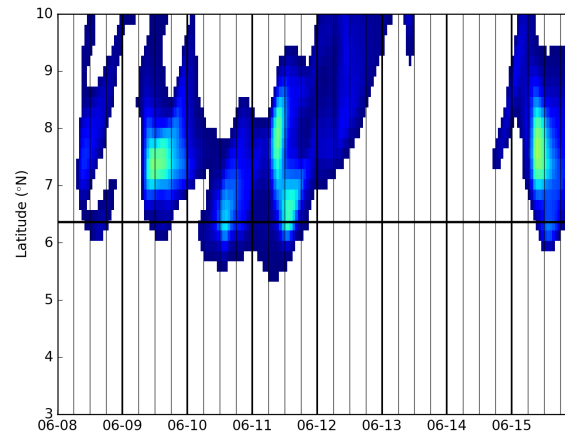
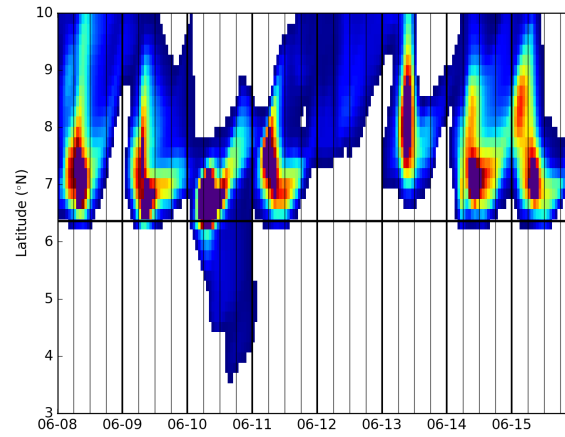


Figure 9. Time-latitude average (Hovmöller) of surface anthropogenic $PM_{2.5}$ concentration ($\mu g\cdot m^{-3}$) averaged along a meridional transect between $2^{\circ}East$ and $3^{\circ}East$ from 1 to 17 June 2016. Black vertical bars delimit the periods of the day (00 UTC; 06 UTC; 12 UTC; 18 UTC). White isocontours present precipitation rate = $3.0 \text{ mm}\cdot\text{hour}^{-1}$. Orange isocontour represents the surface anthropogenic $PM_{2.5}$ concentration = $4 \mu g\cdot m^{-3}$.

a) Cotonou concentrations with Accra (Ghana) emissions



b) Cotonou concentrations with Lome (Togo) emissions



c) Cotonou concentrations with Cotonou (Benin) emissions

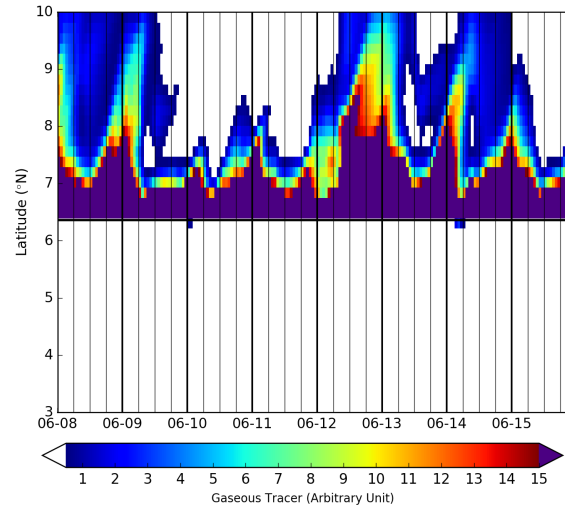


Figure 10. Time-latitude average (Hovmöller) of gaseous tracers concentration (a.u.) averaged along a meridional transect between $2^{\circ}E$ and $3^{\circ}E$ centered on Cotonou (Benin) from 8 to 15 June 2006. Emissions are set up with a constant emission between 0 m and 500 m altitude at: a) Cotonou (Benin), b) Lome (Togo) and c) Accra (Ghana). Black vertical bars delimit the periods of the day (00 UTC; 06 UTC; 12 UTC; 18 UTC).

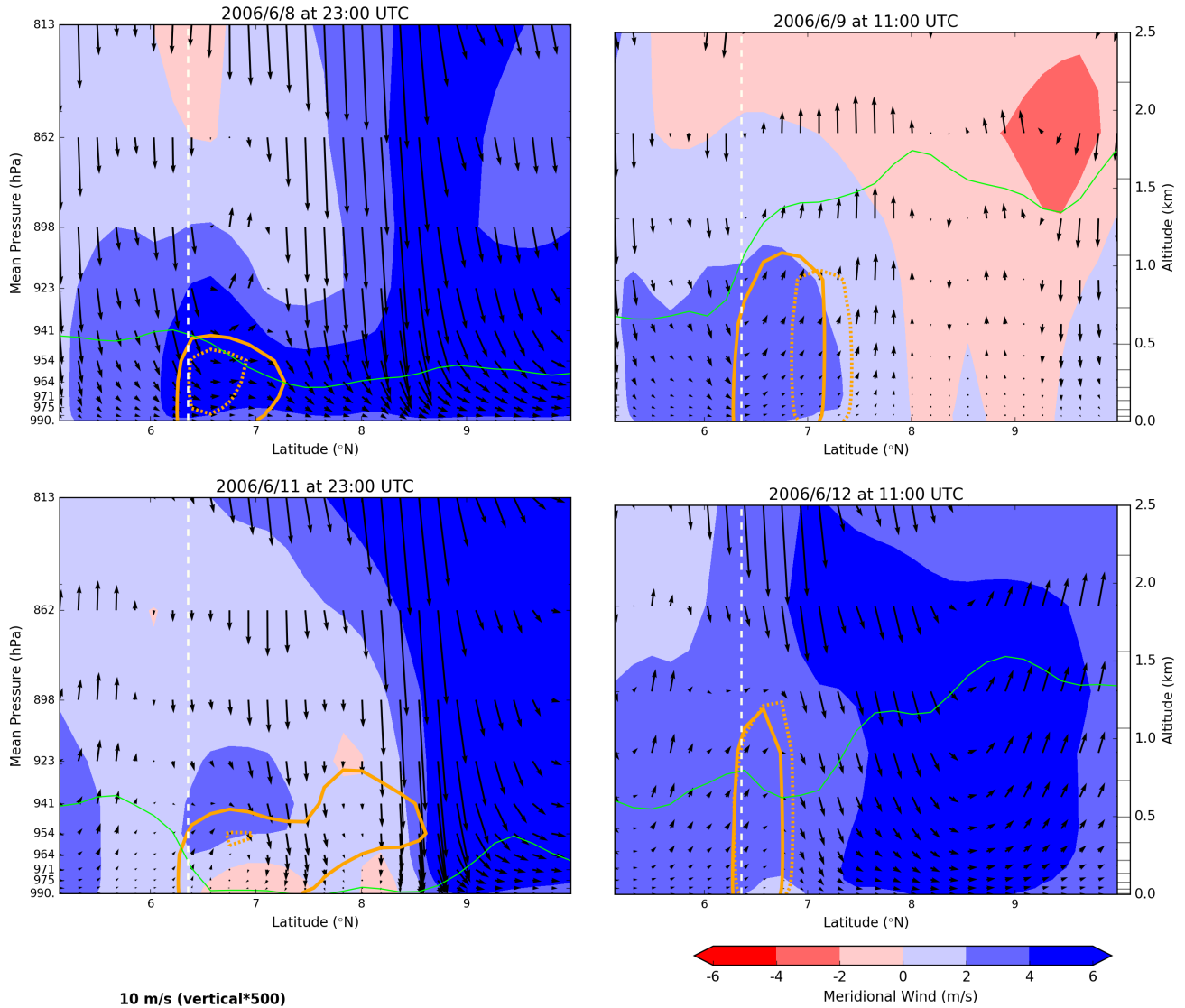


Figure 11. Vertical cross-section of the meridional wind (shading in m.s^{-1}) along a meridional transect from 5°N to 10°N and averaged from 2°E to 3°E including Cotonou (Benin). The two orange isocontours are tracer concentrations released in Cotonou and in Lome, respectively bold and dashed, with same threshold values (in arbitrary unit). Vectors are vertical and meridional represent the wind field in the plan of the transect (with an aspect ratio of 500 between the meridional and the vertical components). The green line is the PBL height (m). The white vertical dash line is the latitude of the coast.

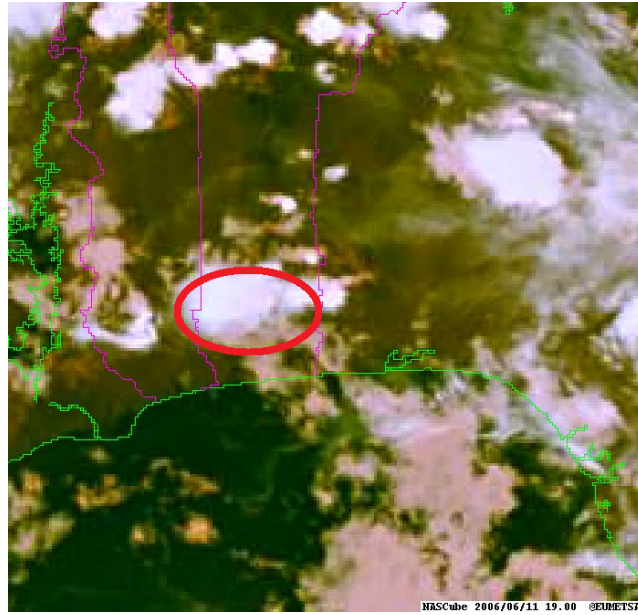


Figure 12. EUMETSAT visible image of the Cotonou area of the 11 June 2006 at 19 UTC (from NAScube (<http://nascube.univ-lille1.fr>)). The red ellipse is the convective cell location.

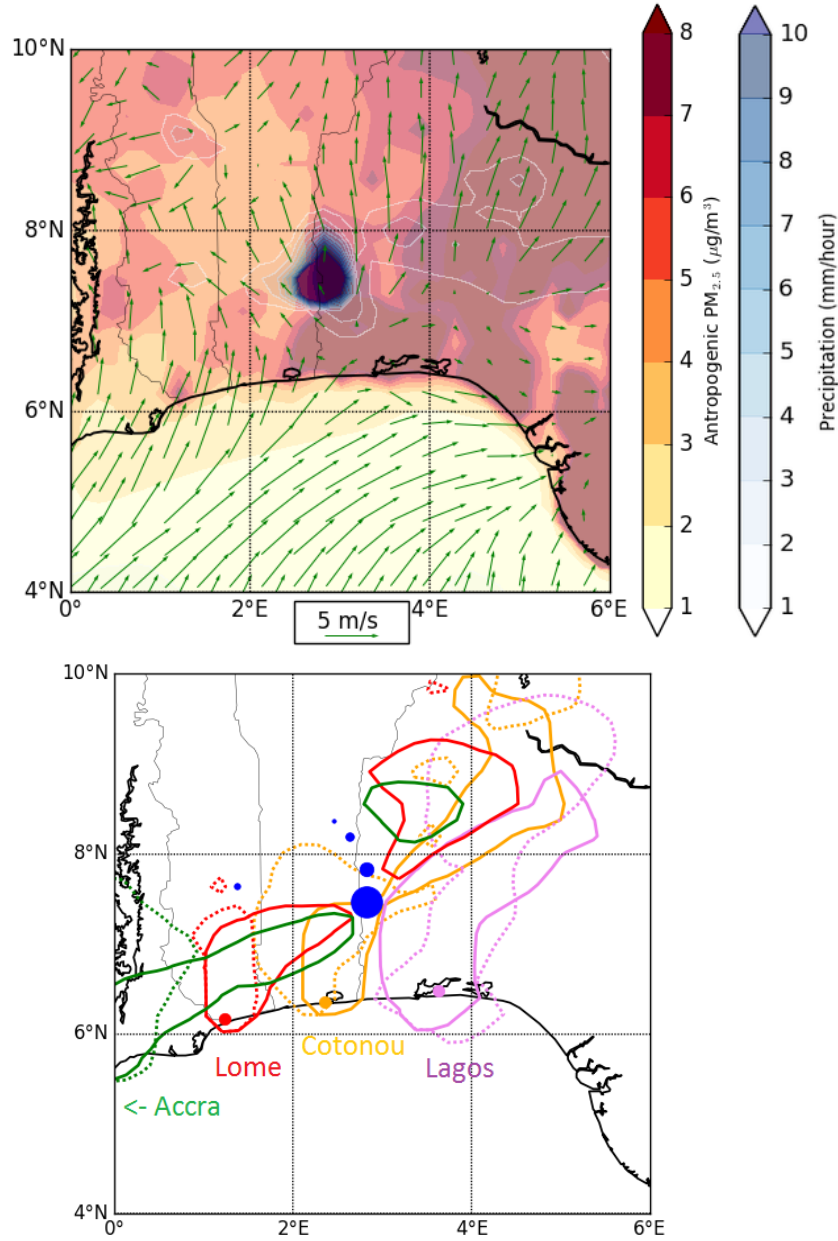


Figure 13. (top) Map of Cotonou area for the 11 June 2006 at 19 UTC–19 UTC with wind vectors at 10 m (green arrows), precipitation (blue shading), anthropogenic PM_{2.5} concentration (red shading); (bottom) Isocontours of tracers concentration on 11 June at 19 UTC (solid line) and on 12 June at 01 UTC (dashed line), released in Accra (Ghana) in green, Lome (Togo) in red, Cotonou (Benin) in orange, Lagos (Nigeria) in violet. Blue dots show precipitation location each hour between 11 June at 19 UTC and on 12 June at 01 UTC (the size of blue dots depends on precipitation amount).

List of Tables

1	Range of 2-minute average modeled and observed concentrations of CO (ppb) and PM _{2.5} (μg.m ⁻³) in the PBL (altitude lower than 1000 m) over three regions: Coastal region (6.3°N - 9.0°N), Sudano-Guinean region (9.0°N - 11.0°N), Sudano-Sahelian region (11.0°N - 13.5°N).	42
5	2 CO (ppb) average and relative contributions (%) of each type of pollution source (background, anthropogenic, fire <u>biomass burning</u>) at Cotonou (Benin), Djougou (Benin) and Niamey (Niger). The time averaged periods correspond to each month of (May, June, July) and to the whole period (from May to July).	43
10	3 PM _{2.5} (μg.m ⁻³) average and relative contributions (%) of type of pollution source (anthropogenic, fire <u>Biomass burning</u> , dust, biogenic, sea salt) at Cotonou (Benin), Djougou (Benin) and Niamey (Niger). The time averaged periods correspond to each month of (May, June July) and to the whole period (from May to July).	44

Pollutants obs/mod	Coastal region			Sudano-Guinean region			Sudano-Sahelian region		
Aircraft observations of 13 June 2006 from 10 UTC to 13 UTC									
	Mean	Min	Max	Mean	Min	Max	Mean	Min	Max
CO CHIMERE (ppb)	207.24	174.90	233.03	231.52	217.50	244.54	243.88	212.25	275.76
CO Aircraft (ppb)	172.78	146.78	209.21	172.51	161.43	182.14	159.26	148.70	174.24
PM _{2.5} CHIMERE ($\mu\text{g.m}^{-3}$)	23.95	19.26	26.01	28.96	25.46	33.87	55.15	35.18	79.93
PM _{2.5} Aircraft ($\mu\text{g.m}^{-3}$)	15.67	7.57	33.02	49.72	22.33	77.88	55.81	34.22	72.20
Aircraft observations of 14 June 2006 from 13 UTC to 16 UTC									
	Mean	Min	Max	Mean	Min	Max	Mean	Min	Max
CO CHIMERE (ppb)	212.71	190.23	239.83	229.15	205.49	246.75	244.74	232.68	257.97
CO Aircraft (ppb)	200.21	185.49	222.34	181.51	153.11	233.35	168.66	146.35	200.66
PM _{2.5} CHIMERE ($\mu\text{g.m}^{-3}$)	42.79	28.23	64.33	82.25	64.43	92.93	84.01	79.65	91.46
PM _{2.5} Aircraft ($\mu\text{g.m}^{-3}$)	39.40	37.26	42.37	39.36	23.60	59.12	92.08	50.11	138.86

Table 1. Range of 2-minute average modeled and observed concentrations of CO (ppb) and PM_{2.5} ($\mu\text{g.m}^{-3}$) in the PBL (altitude lower than 1000 m) over three regions: Coastal region (6.3°N - 9.0°N), Sudano-Guinean region (9.0°N - 11.0°N), Sudano-Sahelian region (11.0°N - 13.5°N).

CO	May-July		May		June		July	
Cotonou (Benin)								
Average (ppb)	221.01		157.25		239.11		267.26	
Background (ppb and %)	73.30	33.17	73.58	46.79	72.82	30.45	73.48	27.50
Anthropogenic (ppb and %)	64.75	29.30	67.83	43.14	64.65	27.04	61.77	23.11
Fire-Biomass burning (ppb and %)	82.96	37.54	15.84	10.07	101.64	42.51	132.00	49.39
Djougou (Benin)								
Average (ppb)	226.78		180.28		240.65		259.85	
Background (ppb and %)	75.27	33.19	77.38	42.92	75.23	31.26	73.21	28.17
Anthropogenic (ppb and %)	80.77	35.62	93.52	51.88	89.01	36.99	60.04	23.11
Fire-Biomass burning (ppb and %)	70.74	31.19	9.38	5.21	76.41	31.75	126.60	48.72
Niamey (Niger)								
Average (ppb)	212.44		171.24		229.26		237.34	
Background (ppb and %)	78.95	37.16	82.72	48.30	78.69	34.32	75.42	31.78
Anthropogenic (ppb and %)	82.54	38.85	83.92	49.01	98.24	42.85	65.96	27.79
Fire-Biomass burning (ppb and %)	50.95	23.98	4.60	2.69	52.33	22.82	95.97	40.43

Table 2. CO (ppb) average and relative contributions (%) of each type of pollution source (background, anthropogenic, **firebiomass burning**) at Cotonou (Benin), Djougou (Benin) and Niamey (Niger). The time averaged periods correspond to each month of (May, June, July) and to the whole period (from May to July).

PM _{2.5}	May-July		May		June		July	
Cotonou (Benin)								
Average (μg.m ⁻³)	29.62		23.31		28.89		36.64	
Anthropogenic (μg.m ⁻³ and %)	3.45	11.64	3.44	14.75	3.44	11.90	3.47	9.46
Fire-Biomass burning (μg.m ⁻³ and %)	12.02	40.58	2.54	10.89	14.38	49.79	19.21	52.44
Dust (μg.m ⁻³ and %)	4.35	14.68	8.89	38.15	2.34	8.10	1.74	4.76
Biogenic (μg.m ⁻³ and %)	6.04	20.38	5.84	25.04	5.68	19.65	6.59	17.98
Salt (μg.m ⁻³ and %)	3.77	12.72	2.60	11.17	3.05	10.56	5.62	15.35
Djougou (Benin)								
Average (μg.m ⁻³)	38.25		41.31		37.71		35.70	
Anthropogenic (μg.m ⁻³ and %)	4.10	10.72	4.38	10.60	4.59	12.16	3.35	9.38
Fire-Biomass burning (μg.m ⁻³ and %)	9.18	23.99	1.34	3.23	9.36	24.82	16.84	47.17
Dust (μg.m ⁻³ and %)	13.55	35.43	23.73	57.44	12.05	31.95	4.83	13.52
Biogenic (μg.m ⁻³ and %)	9.95	26.01	10.76	26.05	10.44	27.68	8.66	24.25
Salt (μg.m ⁻³ and %)	1.47	3.85	1.10	2.67	1.28	3.39	2.03	5.68
Niamey (Niger)								
Average (μg.m ⁻³)	53.76		71.59		52.56		37.09	
Anthropogenic (μg.m ⁻³ and %)	4.22	7.85	4.00	5.58	5.15	9.80	3.54	9.54
Fire-Biomass burning (μg.m ⁻³ and %)	5.73	10.66	0.56	0.78	5.47	10.41	11.15	30.06
Dust (μg.m ⁻³ and %)	36.86	68.57	61.02	85.24	34.34	65.35	15.14	40.83
Biogenic (μg.m ⁻³ and %)	6.31	11.75	5.58	7.79	7.08	13.48	6.31	17.01
Salt (μg.m ⁻³ and %)	0.63	1.18	0.44	0.61	0.51	0.96	0.95	2.56

Table 3. PM_{2.5} ($\mu\text{g.m}^{-3}$) average and relative contributions (%) of type of pollution source (anthropogenic, **fireBiomass burning**, dust, biogenic, sea salt) at Cotonou (Benin), Djougou (Benin) and Niamey (Niger). The time averaged periods correspond to each month of (May, June July) and to the whole period (from May to July).